

ASSESSMENT OF IRRADIATION EFFECTS IN RADWASTE CONTAINING ORGANIC ION-EXCHANGE MEDIA

TOPICAL REPORT

K.J. Swyler, C.J. Dodge, and R. Dayal

May 1984

NUCLEAR WASTE MANAGEMENT DIVISION
DEPARTMENT OF NUCLEAR ENERGY, BROOKHAVEN NATIONAL LABORATORY
UPTON, LONG ISLAND, NEW YORK 11973

Prepared for the
United States Nuclear Regulatory Commission
Office of Nuclear Regulatory Research
Contract No. DE-AC02-75CH00015



8410030353 840930
PDR NUREG
CR-3812 R PDR

ASSESSMENT OF IRRADIATION EFFECTS IN RADWASTE CONTAINING ORGANIC ION-EXCHANGE MEDIA

TOPICAL REPORT

K.J. Swyler, C.J. Dodge, and R. Dayal

Contributors

C.I. Anderson	W. Tremel
W.W. Becker	A.J. Weiss
B.A. Karlin	

Manuscript Completed: March 1984

Published: May 1984

DONALD G. SCHWEITZER, HEAD
NUCLEAR WASTE MANAGEMENT DIVISION
DEPARTMENT OF NUCLEAR ENERGY, BROOKHAVEN NATIONAL LABORATORY
UPTON, NEW YORK 11973

PREPARED FOR THE UNITED STATES NUCLEAR REGULATORY COMMISSION
OFFICE OF NUCLEAR REGULATORY RESEARCH
CONTRACT NO. DE-AC02-76CH00016
FIN NO. A-3236

NOTICE

This report was prepared as an account of work sponsored by an agency of the United States Government. Neither the United States Government nor any agency thereof, or any of their employees, makes any warranty, expressed or implied, or assumes any legal liability or responsibility for any third party's use, or the results of such use, of any information, apparatus, product or process disclosed in this report, or represents that its use by such third party would not infringe privately owned rights.

The views expressed in this report are not necessarily those of the U.S. Nuclear Regulatory Commission.

Available from
GPO Sales Program
Division of Technical Information and Document Control
U.S. Nuclear Regulatory Commission
Washington, D.C. 20555
and
National Technical Information Service
Springfield, Virginia 22161

EXECUTIVE SUMMARY

Recently, regulatory consideration has been devoted to the effects of self-irradiation on radwaste containing organic ion-exchange media. This consideration was prompted by decontamination operations at TMI-II, and by the development of technical positions in support of federal regulation 10 CFR 61. A previous report in this program has described certain aspects of radiation damage to organic ion-exchange media in some detail. The present report treats the practical consequence of these effects on the storage and disposal of radwaste ion-exchange media, and the validity of laboratory test procedures for predicting field performance.

Accelerated testing of ion-exchange media using high-dose-rate external gamma radiation is felt to be a valid procedure for assessing certain aspects of field behavior--i.e. radiolytic scission of the resin functional group, radiolytic gas generation of free liquids and resin agglomeration, provided both the test data and the field conditions refer to storage in a closed environment. For resins irradiated in a sealed environment, there is no evidence that post-irradiation reactions will significantly influence test results. Certain resin decomposition processes appear to depend largely on resin moisture content, and may not be particularly sensitive to resin loading. This has the advantage of generality from the viewpoint of establishing regulatory guidance. Other factors such as the effect of radiation on local pH conditions are sensitive to overall resin loading and may require specific evaluation.

One practical consequence of radiolytic acidity is to promote the corrosion of mild steel in irradiated resin. The corrosion process is complex, probably involving a competition between radiolytic H^+ generation and H^+ uptake in the corrosion process. Consequently, corrosion rates may depend on metal surface-to-bed volume ratio and radiation dose rate. Also, the extent of corrosion cannot be simply bounded by measuring resin pH. Case-specific, long term (i.e. low radiation dose-rate) evaluations might be required if rigorous guidelines to protect radwaste containers against corrosion are required. Certainly, the amount of oxygen expected in the system under field conditions should be well established, if not regulated. For sulfonic acid resins with typical loadings (Na^+) mild radiolytic metal corrosion in a sealed environment was not extreme.

CONTENTS

EXECUTIVE SUMMARY	iii
CONTENTS.	v
FIGURES	vii
TABLES.	ix
ACKNOWLEDGMENTS	xi
1. INTRODUCTION	1
2. EXPERIMENTAL TECHNIQUES.	3
2.1 Mild Steel Corrosion Measurements	3
2.2 Electron Irradiation Studies.	5
3. INTERACTION OF MILD STEEL WITH IRRADIATED RESINS	6
3.1 Effect of Resin Loading on Mild Steel Corrosion in Irradiated Resins.	6
3.2 Effect of Irradiation Dose Rate on Mild Steel Corrosion in Irradiated Resins	10
3.3 Effect of Resin Moisture Content on Mild Steel Corrosion in Irradiated Resins	12
3.4 Effect of Corrosion on Resin Degradation.	17
3.5 Transport of Corrosive Species and Corrosion Products in Resin Beds	22
3.5.1 Chemical Analysis of Corrosion Products in Irradiated Resin Columns	22
3.5.2 Chemical Analysis of Corrosion Products in Resin/Sulfuric Acid Mixtures.	26
3.5.3 Spatial Extent of Resin Blackening Due to Mild Steel Corrosion	29
4. EFFECT OF AGING PROCESSES AND ENVIRONMENTAL CONDITIONS ON RESIN RADIOLYSIS.	32
4.1 Irradiation of IRN-77 Resin Under Vented (Oxic) Conditions. . .	32
4.2 Long-Term Irradiation Studies	35
4.3 Aging Studies on Irradiated Resins and Resin-Water Solutions. .	38
5. ELECTRON IRRADIATION EXPERIMENTS	44
6. SURVEY/CHARACTERIZATION OF FIELD EXPERIENCE WITH HEAVILY-LOADED ION-EXCHANGE MEDIA.	46
6.1 Epicor-II Liners.	46
6.1.1 Epicor II Liner PF-16 Characterization	46
6.1.2 Epicor II Liner PF-3 Characterization.	48
6.2 LDS Resins From TMI-II.	54

CONTENTS (cont.)

7.	DISCUSSION AND SUMMARY	55
7.1	Enhanced Mild Steel Corrosion in Irradiated Ion-Exchange Media.	55
7.2	Comparison of Field Data and Laboratory Results	59
7.2.1	General Observations	59
7.2.2	Epicor-II Liner PF-16.	59
7.2.3	Epicor-II PF-3	60
7.2.4	LDS Resins from TMI-II	61
7.2.5	Summary.	62
7.3	Conclusions and Recommendations	63
8.	REFERENCES	67

FIGURES

2.1	1018 Mild Steel Coupon Before and After 4-Minute Immersion in Clarke's Solution	4
3.1	Weight Loss vs Contact Time for Mild Steel Coupons Irradiated in Contact with Different Forms of IRN-77 Resin.	6
3.2	Weight Loss vs Contact Time for Mild Steel Coupons Irradiated in Contact with IRN-78 OH ⁻ Form Resin.	7
3.3	Weight Loss vs Contact Time for Mild Steel Coupons Irradiated in Contact with Different Forms of IRN-150 Resin	8
3.4	Supernatant pH vs Irradiation Time for IRN-77 Resin With and Without Mild Steel Corrosion Coupons	8
3.5	Supernatant pH vs Irradiation Time for IRN-78 OH ⁻ Form Resin With and Without Mild Steel Corrosion Coupons.	9
3.6	Supernatant and Free Liquid pH vs Irradiation Time for IRN-150 HOH Form Resin With and Without Mild Steel Corrosion Coupons.	9
3.7	Supernatant and Free Liquid pH vs Irradiation Time for IRN-150 NaCl Form Resin With and Without Mild Steel Corrosion Coupons.	10
3.8	Corrosion Weight Loss vs Irradiation Dose for Mild Steel Coupons Irradiated in Contact with Na ⁺ Form IRN-77 Resin	11
3.9	Weight Loss vs Contact Time for Mild Steel Coupons Irradiated in Contact with H ⁺ Form IRN-77 Resins of Different Moisture Content	14
3.10	Weight Loss vs Contact Time for Mild Steel Coupons Irradiated in Contact with Na ⁺ Form IRN-77 Resins of Different Moisture Content	14
3.11	Mild Steel Corrosion Coupons Contacted with Fully Swollen Cation Resin and Cation Resin-Water Slurries During Irradiation at 1.6 x 10 ⁶ rad/hr for 5 Weeks.	16
3.12	pH of Resin-Water Slurries With and Without Corrosion Coupons.	17
3.13	Soluble Sulfate Generation vs Irradiation Dose for IRN-77 Na ⁺ Form Resin With and Without Corrosion Coupons.	18
3.14	Hydrogen Gas Yields vs Corrosion Weight Loss in Mild Steel Coupon Contacted with H ⁺ Form IRN-77 Resin	19

FIGURES (cont.)

3.15	Irradiated IRN-77 Na ⁺ Form Resin with and Without Corrosion Coupons	23
3.16	Growth of Blackened Resin Zone in Irradiated Resin Columns Containing Corrosion Coupons	31
3.17	Growth of Blackened Resin Zone in Resin Columns Containing Corrosion Coupons and Resins Loaded with H ₂ SO ₄	31
4.1	IRN-77 Na ⁺ Form Resin Irradiated to 1.2 x 10 ⁹ rad Under Sealed and Vented Conditions	35
4.2	Supernatant pH vs Irradiation Dose in IRN-77 Resin	36
4.3	Supernatant Sulfate Yields vs Irradiation Dose in IRN-77 Resin	36
4.4	Radiolytic Hydrogen Gas Generation in H ⁺ Form and Na ⁺ Form IRN-77 Resin	37
5.1	Gas Generation in IRN-77 Resin During Electron Irradiation	45
6.1	Epicor-II Liner Core No. 3, 4 in. from Bottom.	49
6.2	Epicor-II PF-3 Liner Core No. 3, 12 in. from Bottom.	49
6.3	Epicor-II Liner Core No. 3, 24 in. from Bottom	50
6.4	Epicor-II Liner PF-3 Core, 18-1/4 in. from Botom	50
6.5	Epicor-II Liner PF-3 Core, 28 in. from Bottom.	51

TABLES

3.1	Effect of Moisture Content on Irradiated and Unirradiated Resins	13
3.2	Radiolytic Hydrogen Yields, Hydrogen Uptake in Corrosion, and Mild Steel Corrosion Weight Loss in Irradiated Resins.	20,21
3.3	Distribution of Corrosion Products and Acidic Species in Irradiated Resin Columns	24
3.4	Distribution of Corrosion Products in Irradiated Resin Columns of Different Height.	25
3.5	Weight Loss for Mild Steel Corrosion Coupon After 10-Day Contact with Resin-H ₂ SO ₄ Solutions	26
3.6	Distribution of Corrosion Products and Acidic Species in Resin Columns Loaded with H ₂ SO ₄	27
4.1	Acidity, Soluble Sulfate and Weight Change for IRN-77 Resin Irradiated Under Vented Conditions	33
4.2	Aging Effects on the Supernatant pH of Irradiated Resin Water Solutions.	38
4.3	Aging Effects on the Supernatant pH of Irradiated Resin Water Solutions.	39
4.4	Aging and Dilution Effects on the Aqueous Supernate pH on Irradiated IRN-77 Resins	40
4.5	Aging and Dilution Effects on the Sulfate Yield in the Supernate Oven Irradiated Cation Resin	40
4.6	Dilution Effects on the Sulfate Yield in the Supernate Over Irradiated Cation Resins of Different Moisture Content	41
4.7	Aging Effects on the Sulfate Yield in the Supernate Over Irradiated Cation Resin.	41
4.8	Comparison of Sulfate Yields in Resin Supernates and Rinses.	42
4.9	Aging Effects on the pH and Sulfate Ion content of Aqueous Supernate of IRN-77 H ⁺ Resin	43
5.1	Hydrogen Ion Concentration (as pH) of Water in Contact with Irradiated Ion Exchange Resins	45
6.1	Properties of Ion-Exchange Media in Epicor-II Liner PF-16.	47

TABLES (cont.)

6.2	Properties of Ion-Exchange Media in Epicor-II Liner PF-3	53
6.3	Decomposition Products in Liquids and Solids (Resins) from the B2 Letdown Demineralizer System at TMI-II.	54
7.1	Estimated average penetration of mild steel by corrosion in resins irradiated to a dose of 10^9 rad	58

ACKNOWLEDGMENTS

The authors would like to acknowledge helpful technical discussion with Dr. P. L. Piciulo, Dr. E. P. Gause, Dr. D. R. MacKenzie, Dr. H. Isaacs and Dr. R. E. Davis. The work of Dr. T. Gangwer merits special mention in focusing attention on the issue. The cooperation of personnel at General Public Utilities (G. Quinn, D. Chung, R. Ogle) and at Batelle Columbus Laboratories (D. Yesso, N. Wynhoff, V. Pasupathi) in providing samples and information is gratefully acknowledged. Finally, the authors would like to express their appreciation of the editorial efforts of S. Bennett, N. Yerry, and E. Pinkston, and thank Dr. D. G. Schweitzer for a critical reading of the manuscript. We would also like to thank the NRC program manager, Dr. Kyo Kim, for his comments.

1. INTRODUCTION

Brookhaven National Laboratory (BNL), under contract to the United States Nuclear Regulatory Commission (NRC), has carried out a research program entitled Characterization of TMI-Type Wastes and Solid Products. This effort was stimulated by questions arising from the use of organic ion-exchange resins in decontamination operations at TMI-II. The objective of this program is to develop a data base applicable to NRC licensing consideration for the storage and disposal of organic ion-exchange resins subjected to high internal irradiation doses as a result of heavy radionuclide loadings.

Irradiation is known to affect the properties of organic ion-exchange resins. The possible impact of radiation effects on the storage and disposal of ion-exchange resins have been considered by a number of workers, notably Gangwer and his colleagues: (Gangwer, Goldstein and Pillay, 1977; Gangwer and Pillay, 1981; McFarland, 1981; Pillay, 1982; Barletta, Swyler and Chan 1982, Swyler and Barletta, 1982; Swyler, Dodge and Dayal, 1982; Sheff, 1982; Capolupo and Sheff, 1982; Gangwer and Pillay 1983; Godbee et al., 1981; United Nuclear Corp., 1982, MacKenzie et al., 1983; Yesso et al., 1982; Wynhoff and Pasupathi, 1983). Most of these studies are based on irradiation damage experiments in the laboratory and do not always allow a quantitative evaluation of radiation effects under field conditions, which may differ significantly from the laboratory. A major thrust of the present program is to first, identify those factors which may affect the correlation between laboratory irradiation damage experiments and field performance, and second, to specify those experimental procedures and empirical methods which can be applied in the laboratory to provide a realistic estimate of the significance of radiolysis effects on radwaste under field conditions.

The first phase of this program involved a parametric study of radiolysis effects on polystyrene-divinyl benzene based ion exchangers. External variables included resin loading, moisture content, irradiation dose and dose rate. Results, including some mechanistic observations, have been described in a previous topical report (Swyler, Dodge and Dayal, 1983).

In the second phase of the program certain practical consequences of these radiolysis effects, including the corrosion of mild steel in irradiated resins, are considered further. These experiments are described in the present report. In addition, experimental techniques which best reflect field behavior are addressed in some detail--the equivalence of various methods for determining the (time-dependent) yields of radiolysis products is examined. Further, accelerator electron irradiations are described to study the correspondence between external gamma vs beta irradiation.

In a separate section of the report, characterization studies on actual field samples of irradiated resins are reviewed. To the extent possible, the correspondence between these results and predictions based on laboratory data is discussed. Finally, based on the considerations above and on information contained in the earlier topical report (Swyler, Dodge and Dayal, 1983), general procedures for evaluating the effects of radiolysis on the disposal

of dewatered ion-exchange resins are recommended. These recommendations are discussed in light of existing NRC guidelines and practices (MacKenzie et al., 1983).

2. EXPERIMENTAL TECHNIQUES

Experimental techniques have been described previously for the most part (Swyler, Dayal and Dodge, 1983). Most measurements refer to irradiation of various forms (chemical loadings) of cation resin (Amberlite, IRN-77), anion resin (Amberlite IRN-78) and mixed bed resin (Amberlite IRN-150) carried out in sealed pyrex vessels. Unless otherwise indicated the resins were irradiated in fully swollen (drip-dry) form. Experiments described in this report involved measurements of mild steel corrosion in irradiated resins, and irradiations with fast electrons. Methods are discussed below.

2.1 Mild Steel Corrosion Measurements

Samples of 1018 steel* were typically rolled to ~0.5 mm thickness and cut to a size of 3.2 cm long and 0.64 cm wide. The coupons were then cleaned and stored in acetone until ready for use. Immediately before insertion into the resin, the coupons were weighed to four significant figures. Generally samples of coupons in contact with 6 g of resin were prepared in glass test tubes (12 mm-diam by 125 mm-long). These tubes were flame sealed to prevent air intrusion or moisture loss, then tapped several times to ensure packing of the resin beads about the coupons. In some measurements, the coupons were placed in 2 g of resin in a 15 mm diameter by 125 mm test tube left unsealed.

In several experiments, disc samples 1.1 cm in diameter x 3.1 mm thick were stamped from 1018 steel sheet stock. These were then contacted with either the top or bottom of a resin column to study transport processes in corrosion.

Irradiation was performed at BNL's gamma irradiation facility. The shielding water of the pool is kept constant at 10°C. However, during irradiation, samples are warmed to roughly room temperature.

Generally, upon removal from the irradiated resin, the coupon was photographed in the corroded state, followed by removal of the corrosion layer by vigorous stirring in Clarke's solution for 3-4 minutes. The coupon was then rinsed with acetone, reweighed, and a photograph of the cleaned sample taken. Two grams of the irradiated resin are withdrawn from the test tube and placed in contact with 10 mL of deionized water. After approximately one day, the pH of the solution is determined. As a point of interest, a pristine uncorroded coupon was photographed in its initial state and again after 4 minutes immersion in Clarke's solution (Figure 2.1). Note that attack of the base metal is minimal. This was confirmed by weight loss measurements, carried out for pristine coupons contacted with Clarke's solution for times of 8, 16, and 24 minutes. These data indicate that the minimum detectable weight change due to corrosion is ~0.0005 g.

*Sanyu Cold Finished Steel Co., LTD., Hiracata City, Osaka, Japan.

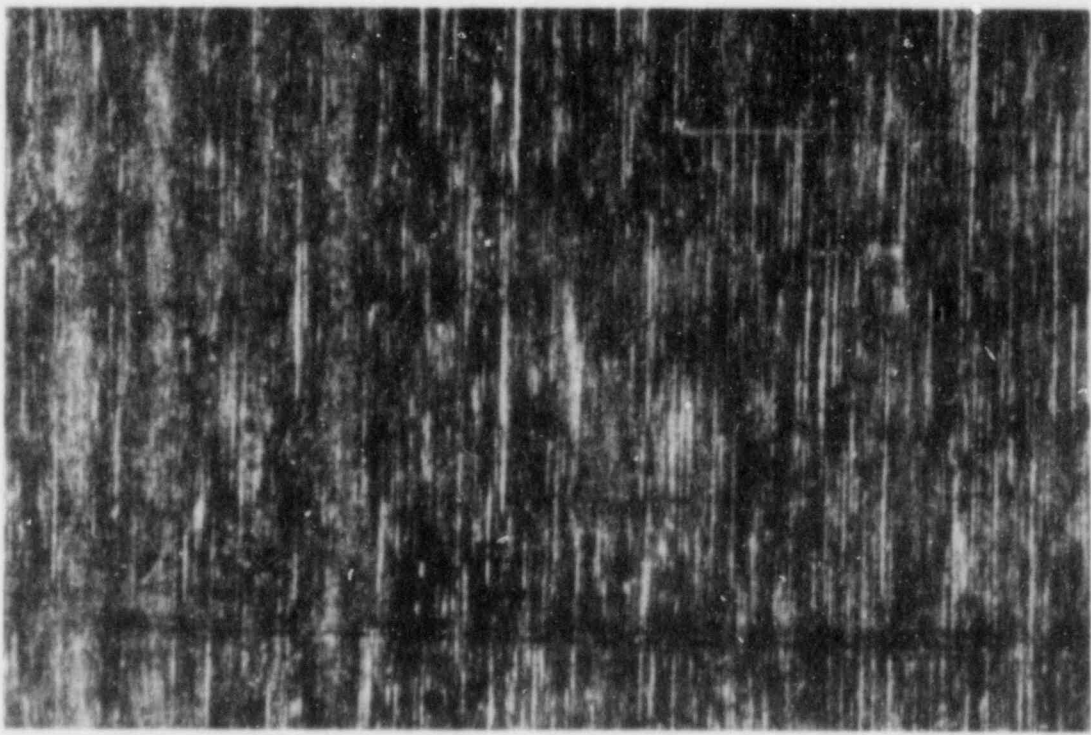
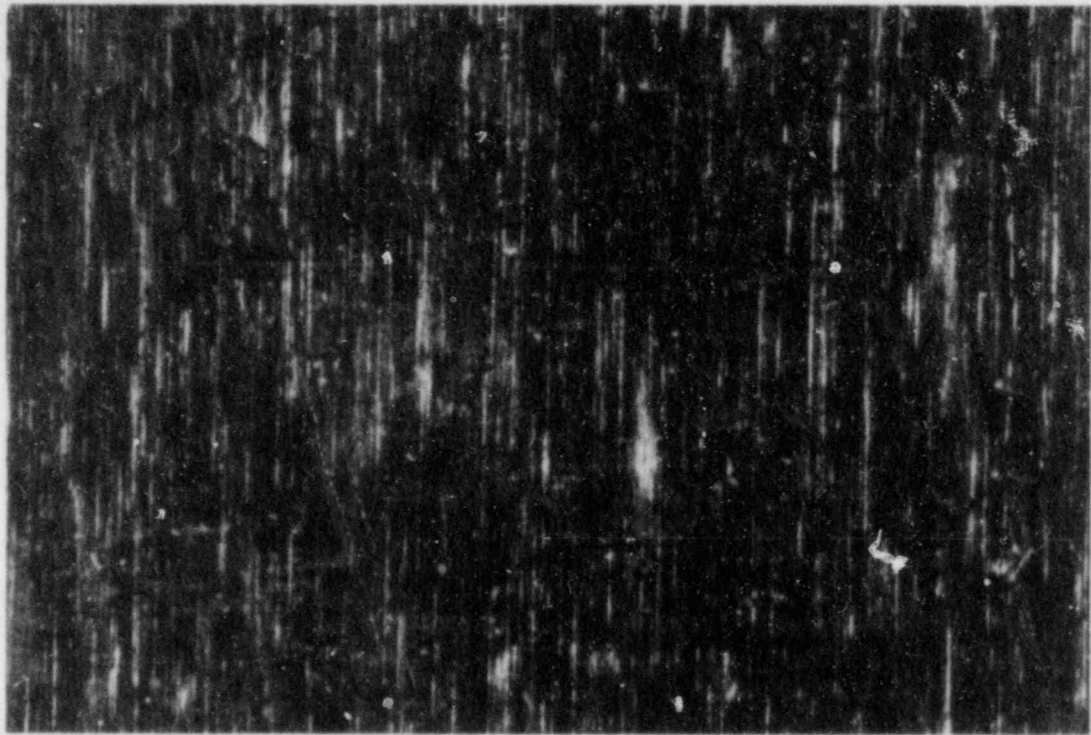


Figure 2.1 1018 mild steel coupon before (top) and after (bottom) 4-minute immersion in Clarke's solution.

2.2 Electron Irradiation Studies

To examine the equivalence of gamma-ray and electron irradiation in producing resin decomposition, samples of IRN-77 resin were irradiated with fast electrons. The irradiations were carried out at BNL's Dynamitron Accelerator. Samples of as-delivered IRN-77 resin were placed in thin walled sample chambers constructed from 304 stainless steel. The sample chambers were rectangular, (2.5 cm x 2.5 cm x 0.5 cm) and all joints were welded. Irradiations were carried out by placing the sample chamber, containing the resin sample, with its large cross section perpendicular to the electron beam axis. The electron beam impinges on the sample cell through thin windows in the accelerator vacuum beam line.

Operating at 2 MeV, the incident electrons are sufficiently energetic to produce a roughly uniform energy deposition along the thin (0.5 cm) dimension of the sample. The electron beam is magnetically steered (rastered) over the large face of the sample cell to produce a uniform irradiation, and the total beam current is monitored by means of a Faraday cup. The maximum dose rate is limited by beam heating effects. Sample temperature during irradiation is monitored by a thermocouple penetrating into the resin column, and air cooling of the sample chamber is accomplished with muffin fans. For electron beam currents of about 3 μ A, a sample temperature of $<40^{\circ}\text{C}$ can be easily maintained. The effective dose rate under this condition is calculated to be approximately 10^8 rad/h (Swyler and Barletta, 1982).

The irradiations were carried out under both vented and sealed conditions. In the latter configuration, the pressure, developed within the cell, can be continuously monitored with a strain gauge pressure transducer, both during and after irradiation. Following irradiation, the resin is removed from the sample cell for subsequent characterization. For irradiation in sealed cells, gas samples were withdrawn for mass spectrographic analysis.

3. INTERACTION OF MILD STEEL WITH IRRADIATED RESINS

Experiments on radiation-induced corrosion described in this section were carried out in order to provide a basis for estimating the lifetime of mild steel containers for dewatered resin wastes. This involved determining corrosion rates for a variety of radiation dose rates, resin loadings and irradiation environments. Measurements were also carried out to determine if corrosion would be retarded by localized depletion of corrosive species within the resin bed. Finally, comparative measurements were carried out to learn if interaction with corrosion products would accelerate or retard radiolytic resin degradation. Results of these studies are described below.

3.1 Effect of Resin Loading on Mild Steel Corrosion in Irradiated Resins

Corrosion rates depend both on resin functionality and on resin loading. Weight loss data for mild steel coupons contacted with different forms of IRN-77 cation resin during irradiation are shown in Figure 3.1. These data refer to fully swollen resin, irradiated in a sealed environment, at 1.6×10^6 rad/h. Weight loss data for mild steel coupons irradiated in contact with IRN-78 anion resin and IRN-150 mixed bed resin are shown in Figures 3.2 and 3.3. These data again refer to fully swollen resin irradiated in a sealed environment at 1.6×10^6 rad/h.

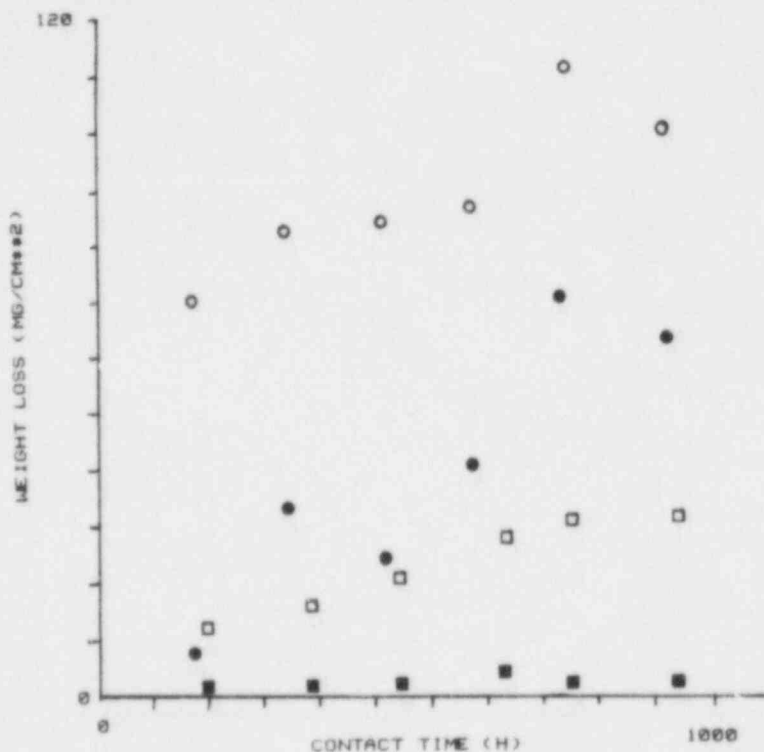


Figure 3.1 Weight loss vs contact time for mild steel coupons irradiated in contact with different forms of IRN-77 resin. ○ -H⁺ form; □ - Na⁺ form. Open points--irradiated at 1.6×10^6 rad/h. Solid points--unirradiated control sample.

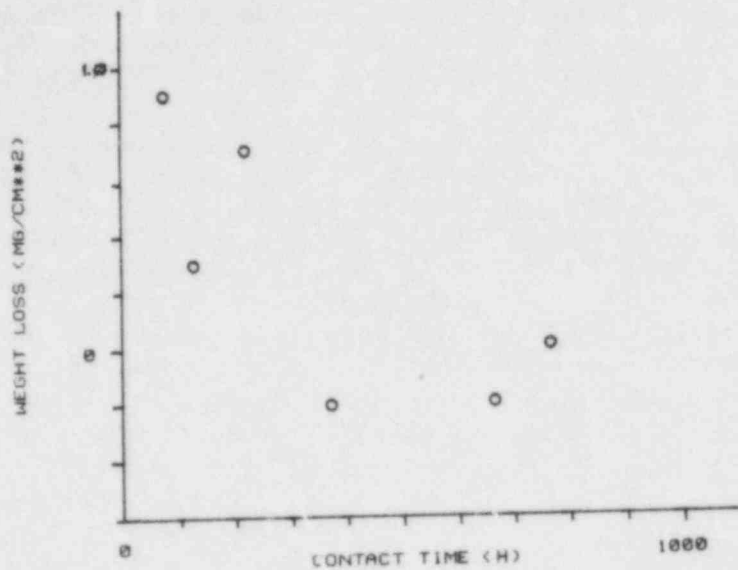


Figure 3.2 Weight loss vs contact time for mild steel coupons irradiated in contact with IRN-78 OH⁻ form resin, irradiated at 1.6×10^6 rad/h.

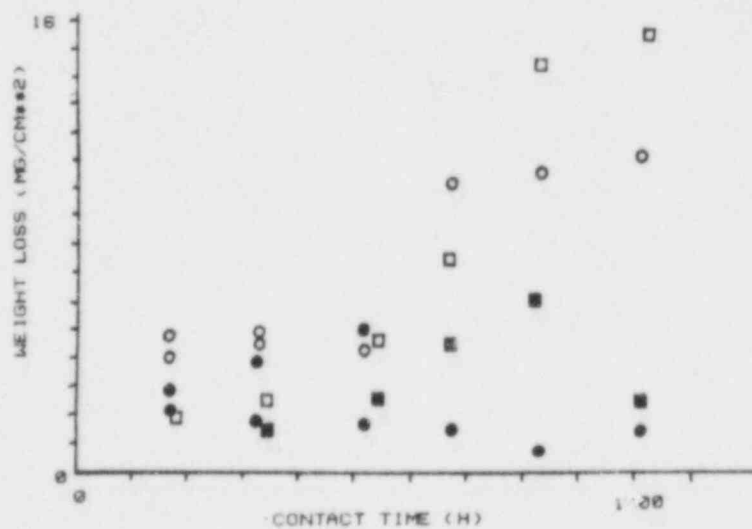


Figure 3.3 Weight loss vs contact time for mild steel coupons irradiated in contact with different forms of IRN-150 resin o - HOH form; □ - NaCl form. Open points--Irradiated at 1.6×10^6 rad/h. Solid points--unirradiated control samples.

Corrosion weight loss is greatest in the H^+ form cation resin, and lowest in the OH^- form anion resin. It should be noted, however, that even unirradiated H^+ form cation resin shows considerable corrosion weight loss. The mixed bed system represents an intermediate case. The Na^+ form cation resin also exhibits corrosion weight loss upon irradiation, relative to the unirradiated specimen.

The corrosive attack on the mild steel can be correlated with the radiolytic formation of acidic species in the resins. Supernate and free liquid pH values are compared for irradiated resins with and without corrosion coupons in Figures 3.4 to 3.7. The pH was determined in the supernate formed by contacting 2g of irradiated resin with 10 mL of deionized water. Irradiation of anion and mixed bed resins alone was found to promote the release of a free liquid phase, based on an earlier study (Swyler, Dodge and Dayal, 1983). For anion and mixed bed resins, the free liquid pH was determined first. The free liquid was then removed by centrifuge, and 10 mL of deionized water was added to 2g of the remaining resin. The supernate pH of this mixture was then measured.

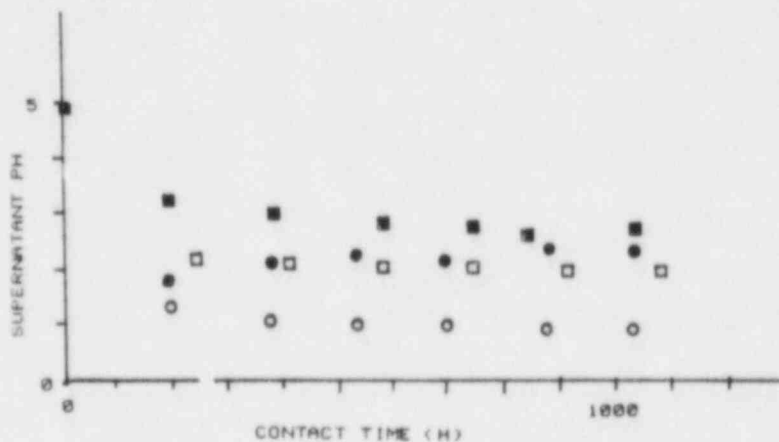


Figure 3.4 Supernatant pH vs irradiation time for IRN-77 resin with (solid points) and without (open points) mild steel corrosion coupons. o - H^+ form resin; \square - Na^+ form resin.

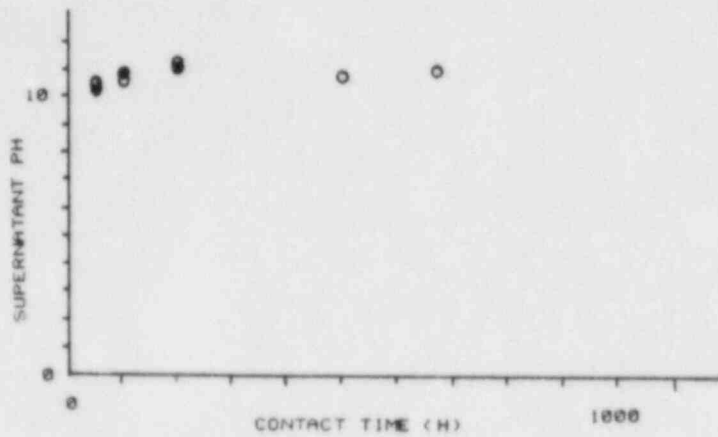


Figure 3.5 Supernatant pH vs irradiation time for IRN-78 OH⁻ form resin with (solid points) and without (open points) mild steel corrosion coupons.

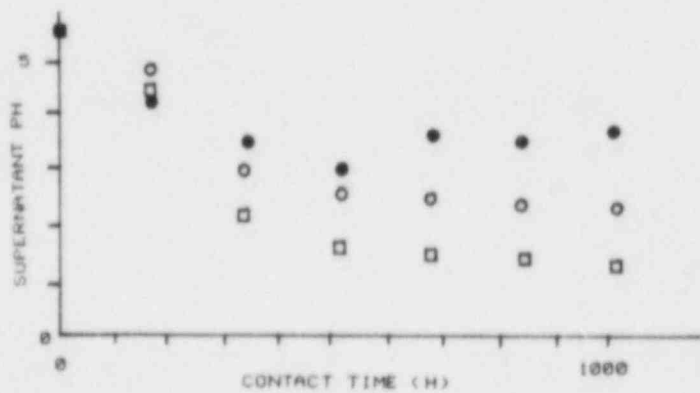


Figure 3.6 Supernatant and free liquid pH vs irradiation time for IRN-150 HOH form resin with (solid points) and without (open points) mild steel corrosion coupons. □ = free liquid; o = supernate over centrifuged resin.



Figure 3.7 Supernatant and free liquid pH vs irradiation time for IRN-150 NaCl form resin with (solid points) and without (open points) mild steel corrosion coupons □ = free liquid; ○ = supernate over centrifuged resin.

The acidity of cation and mixed bed resins is obviously reduced in the mild steel corrosion process. For the basic OH^- form cation resin, mild steel corrosion was not observed. Corrosion rates are greatest for the most acidic resin--the H^+ form. Irradiation induced corrosion is reduced when H^+ form cation resin is mixed with OH^- form cation resin. In a mixed bed, mild steel corrosion did not occur in the unirradiated resin. Corrosion did occur in the mixed bed, however, when acidic conditions were produced by radiolysis.

It is clear that enhanced mild steel corrosion in irradiated resins involves an interaction between the metal and the acidic species produced by irradiation of the resin.

3.2 Effect of Irradiation Dose Rate on Mild Steel Corrosion in Irradiated Resins.

Corrosion weight loss data for mild steel coupons contacted with Na^+ form IRN-77 resin during irradiation at different dose rates are given in Figure 3.8.

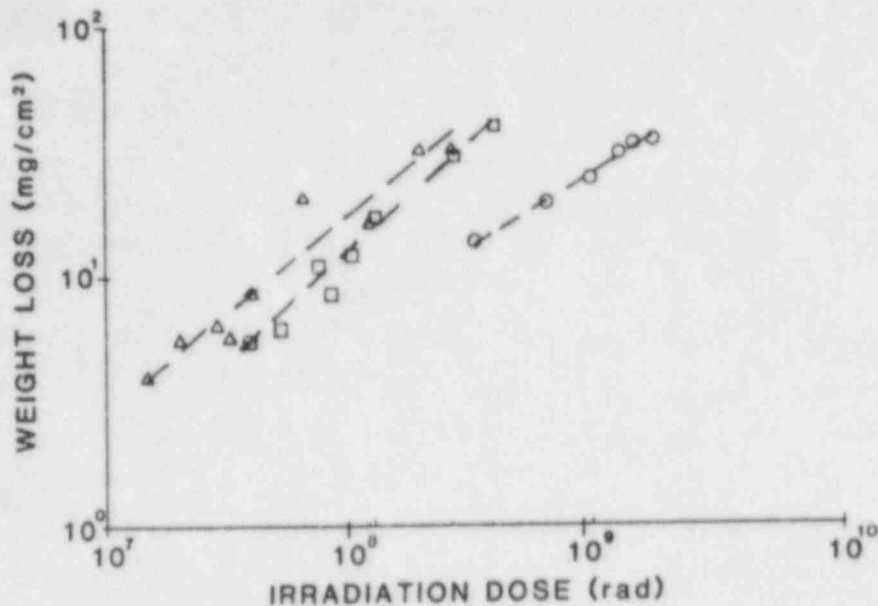


Figure 3.8 Corrosion weight loss vs irradiation dose for mild steel coupons irradiated in contact with Na^+ form IRN-77 resin. Dose rate (rad/h) $\circ = 1.7 \times 10^6$; $\square = 1 \times 10^5 - 8 \times 10^4$; $\Delta = 4 \times 10^4 - 3.5 \times 10^4$.

The data refer to fully swollen samples irradiated in a closed environment, similar to that in Figure 3.1 - 3.7.

For a given irradiation dose, corrosion is greater at low irradiation dose rates. There is no evidence that the yield or G-value for the formation of acidic species depends strongly on irradiation dose rate (Swyler, Dodge and Dayal, 1983; see also Section 4 of this report). Consequently, the relatively greater corrosion per unit dose at lower dose rates probably reflects the longer contact times per unit dose.

At 1.6×10^6 rad/h the weight loss data can be reasonably well described by an expression of the form

$$W = C_1 t^{0.61} \quad (3.1)$$

where W is the weight loss, t is the contact time and C_1 is a constant with. At 1×10^5 rad/h and 4×10^4 rad/h the data are more scattered. The best fit suggests a more nearly linear increase of weight loss with time

$$W = C_2 t^{0.87} \quad (3.2)$$

There is an important distinction between the behavior indicated by Equations 3.1 and 3.2: At high dose rates (Equation 3.1) corrosion rates apparently decrease with time, at lower dose rates Equation 3.2 suggests that corrosion rates remain nearly constant as time proceeds.

3.3 Effect of Resin Moisture Content on Mild Steel Corrosion in Irradiated Resins.

Both the nature and the extent of corrosive attack on mild steel are influenced by resin moisture content. Table 3.1 gives data derived from early scoping experiments on mild steel corrosion in irradiated resins which had been air-dried to different moisture content. In these experiments, coupons were contacted with H^+ and Na^+ form IRN-77 resin and irradiated to 3×10^8 rad in vented tubes.

The supernate pH data clearly indicate that potentially acidic species were formed by irradiation at all moisture contents. In the fully swollen resins, this acidity produced a significant increase in corrosion. In the driest resins with lowest moisture content, no corrosion was observed. It is also worth pointing out that, in these experiments, for fully swollen Na^+ form resins, the corrosion weight loss is greater than that shown in Figure 3.1 for Na^+ form resin at corresponding radiation dose. This difference may reflect different experimental conditions--data in Figure 3.1 refer to resin irradiation in a closed environment, while the data in Table 3.1 were obtained on resin irradiated in open tubes. A second reason for this difference may be in the resin loading itself. The pH of the Na^+ form resin used in this scoping experiment was constantly lower than that of the material used in later experiments, suggesting that the H^+ to Na^+ form resin conversion was incomplete in the resin used in the scoping measurements.

Table 3.1

Effect of Moisture Content on Irradiated and Unirradiated Resins

Resin Form	Percent Moisture	pH of D.I.W. Resin/Mixtures	Coupon Percent Weight Loss
<u>Unirradiated</u>			
H ⁺	55	2.8, 3.2, 3.1	9, 5, 6
	27	3.3, 3.1	2, 4
	14	3.2, 3.3	0, 0
Na ⁺	50	3.6, 3.5, 3.5	4, 4, 4
	25	3.5, 3.4	1, 1
	13	3.3, 3.5	0, 0
<u>3 x 10⁸ rad</u>			
H ⁺	55	top 1.7, 1.6	20, 8
		bottom 1.5	
	27	top 1.5, 1.3	4, 7
		bottom 1.4, 1.4	
	14	top 1.6, 1.5	0, 0
		bottom 1.5, 1.5	
Na ⁺	50	top 2.5, 2.3	4, 5
		bottom 2.8, 2.6	
	25	top 2.3, 2.2	2, 3
		bottom 2.5, 2.4	
	13	top 2.4, 2.4	0, 0
		bottom 2.4, 2.4	

Contact times for corrosion experiments:

Unirradiated samples: 190 h

Irradiated samples:

50-55% moisture: 78 h unirradiated + 75 h irradiated.

25-27% moisture: 75 h unirradiated + 75 h irradiated.

13-14% moisture: 6 h unirradiated + 75 h irradiated.

Corrosion weight loss vs contact time is shown for mild steel coupons irradiated in resin under various moisture conditions in Figures 3.9 and 3.10.

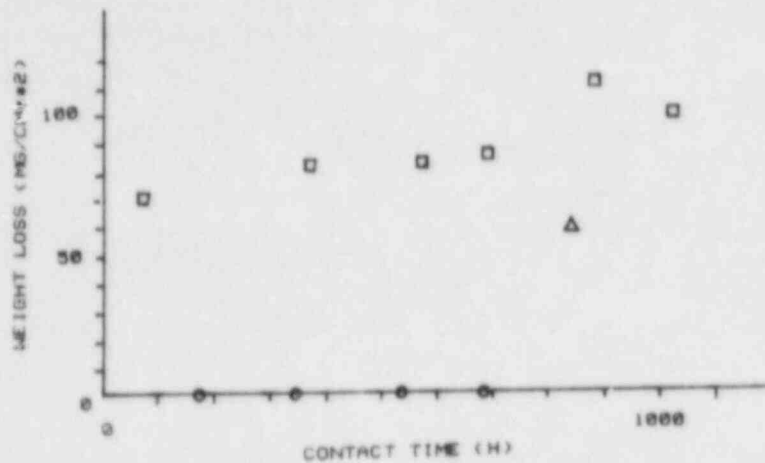


Figure 3.9 Weight loss vs contact time for mild steel coupons irradiated in contact with H^+ form IRN-77 resins of different moisture content. Δ = oven dry resin (7% moisture); \square = fully swollen resin (52% moisture); 2 g resin in 10 mL deionized water. Irradiated at 1×10^6 rad/h.

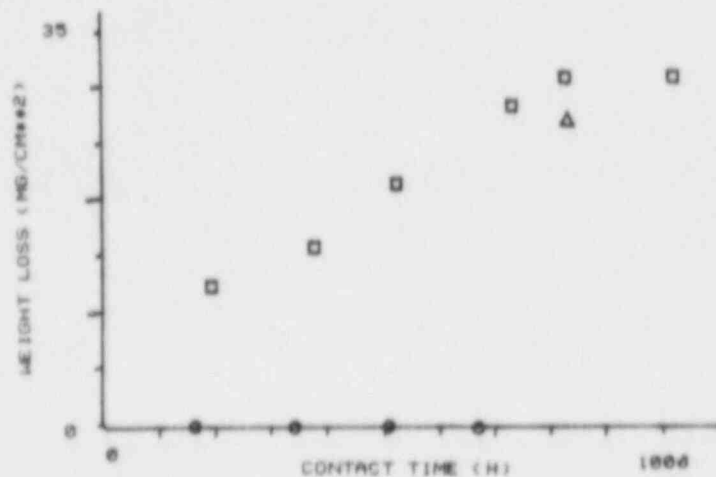


Figure 3.10 Weight loss vs contact time for mild steel coupons irradiated in contact with Na^+ form IRN-77 resins of different moisture content. Δ = oven dry resin (7% moisture); \square = fully swollen resin (52% moisture); 6 g resin in 30 ml deionized water. Irradiated at 1.6×10^6 rad/h.

As in the scoping measurements, corrosion based on weight loss, is undetectable in the dry resins. Interestingly, where comparison is possible, the corrosion weight loss in the irradiated H^+ form resin-water solution is lower than that for coupons contacted with fully swollen resin. Also, there is a difference in the mode of corrosive attack. In coupons contacted with fully swollen resin, corrosion is characterized by extensive pitting (Figure 3.11, upper). In resin-liquid slurries, (Figure 3.11, lower) corrosion is somewhat more uniform. Also a line is apparent on the coupons at the resin-liquid interface possible denoting a boundary between anodic and cathodic regions (Scully, 1975). Overall the data indicates that corrosion processes may proceed somewhat differently in fully swollen resins and resin-liquid slurries. This fact will be considered when further comparing corrosion in fully swollen cation resin with corrosion in mixed bed systems where free liquid is released.

pH data on irradiated resin-water slurries with and without corrosion coupons are shown in Figure 3.12.

The irradiated slurry pH is increased for samples containing corrosion coupons. The effect is similar to that observed in the supernate of fully swollen resins and further suggests that acidic species are taken up or neutralized in the corrosion process. Another possibility, that the presence of corrosion products inhibits the formation of acidic species, is considered further in the next section.

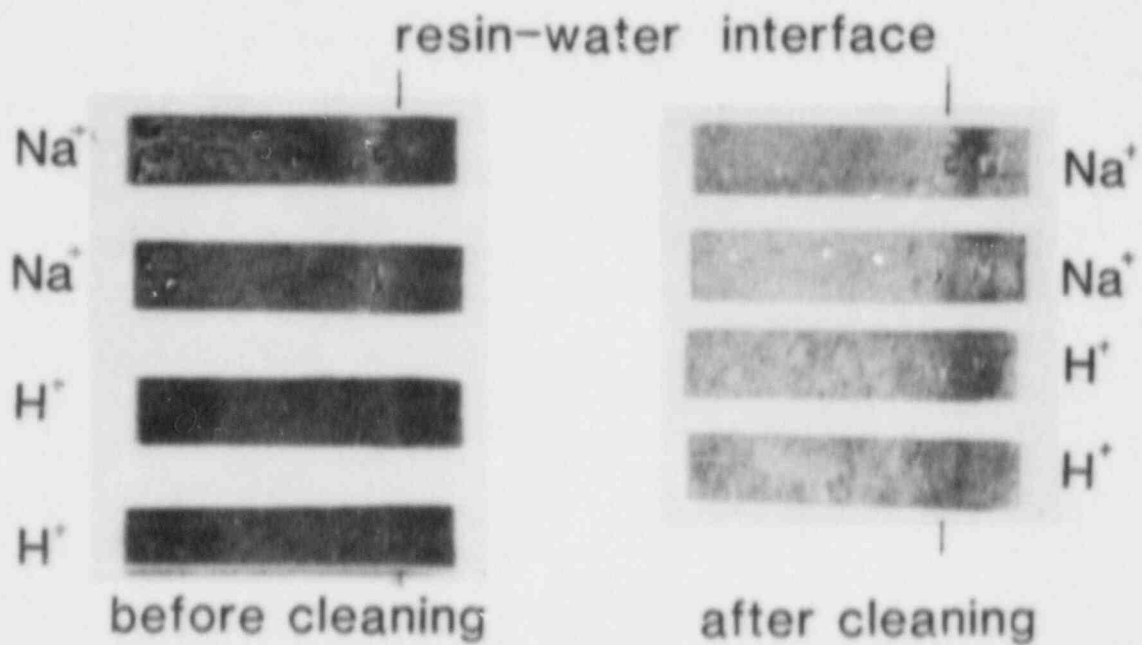
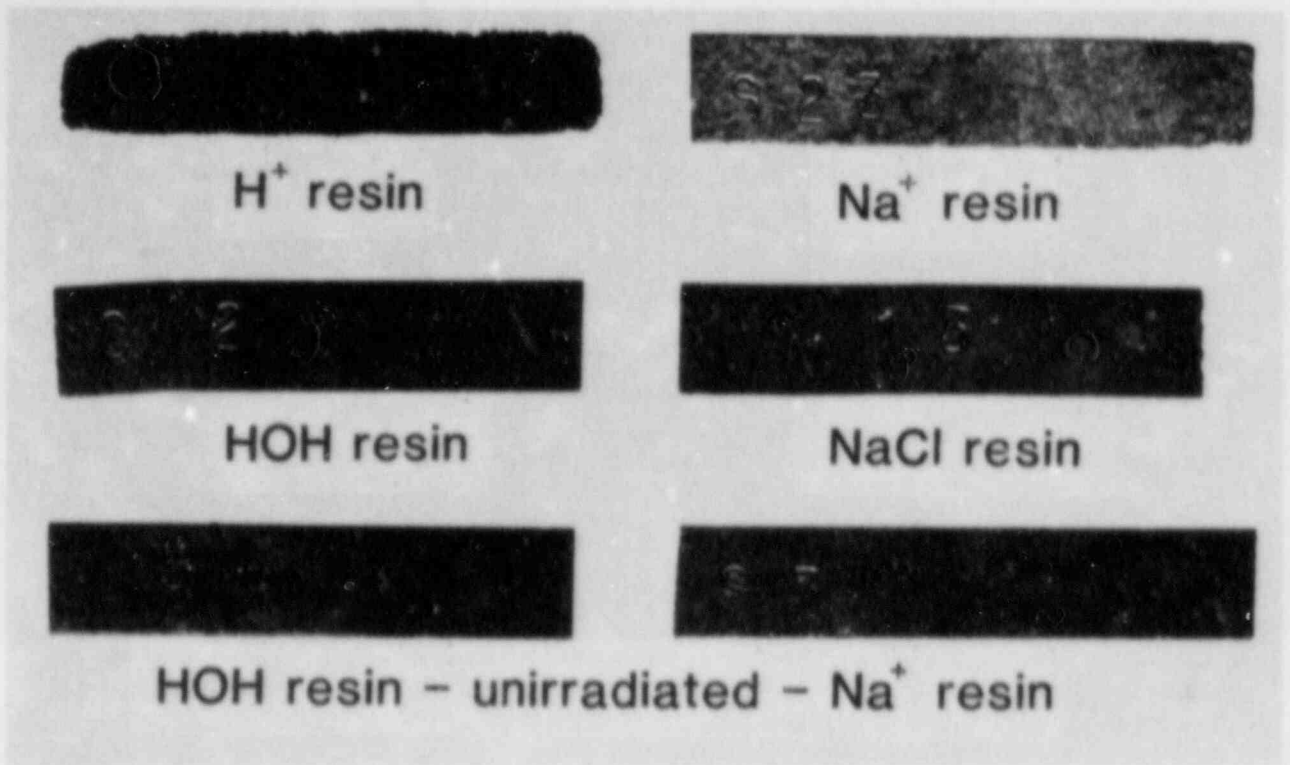


Figure 3.11 Mild steel corrosion coupons contacted with fully swollen cation resin (upper) and cation resin-water slurries (lower) during irradiation at 1.6×10^6 rad/yr for 5 weeks. Unirradiated control coupons are also shown.

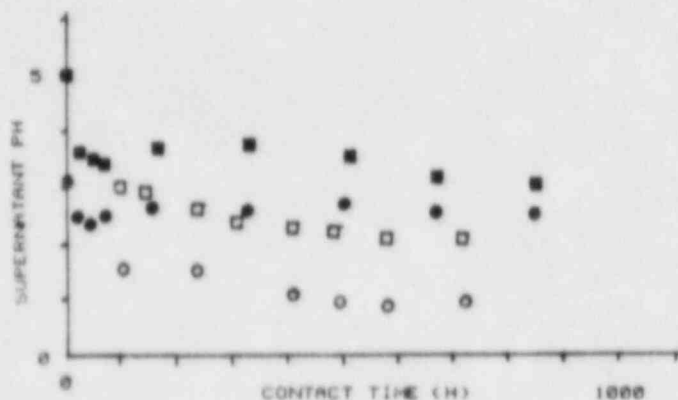


Figure 3.12. pH of resin-water slurries (29 resin/10 ml. DIW) with and without corrosion coupons. Irradiated at 1.6×10^6 rad/h. \square = H^+ form resin \circ = Na^+ form resin. Solid points - with corrosion coupons. Open points - no corrosion coupon.

3.4 Effect of Corrosion on Resin Degradation

In sulfonic acid cation resin, radiolytic acid formation is due largely to radiolytic scissions of the SO_3^- functional group (Swyler, Dodge and Dayal, 1983). This process can be monitored by determining the amount of free sulfate ion released when irradiated resins are contacted with deionized water. By this measure, radiolytic scission of the resin functional group is not grossly affected by the corrosion process. Figure 3.13 shows that radiolytic sulfate yields differ by less than 50% for cation resin samples irradiated with and without corrosion coupons.

The radiolytic processes which originally produced acid conditions in the resin are apparently not suppressed by interaction with corrosion products.* Consequently the relatively greater pH for samples containing corrosion coupons apparently indicates that radiolytic H^+ is taken up or neutralized in the corrosion process.

*Since the pH and sulfate values refer to a volume of resin which is large compared to the corrosion coupon, it is possible that local effects at the resin/coupon interface may be somewhat obscured in the bulk measurement.

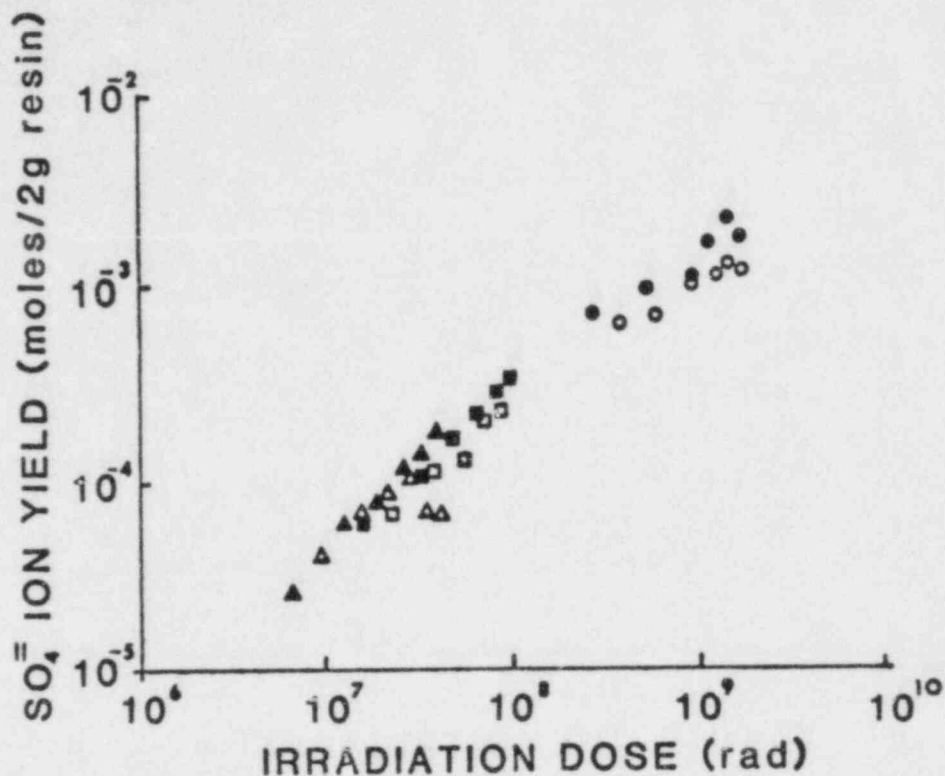


Figure 3.13 Soluble sulfate generation vs irradiation dose for IRN-77 Na⁺ form resin (2 g) with and without corrosion coupons. Dose rates (rad/h): o = 1.7 × 10⁶; □ = 1 × 10⁵; Δ = 4 × 10⁴. Solid points--sample with corrosion coupon; open points--sample without corrosion coupon.

Some of the radiolytic H⁺ may be converted to H₂ in the corrosion process. This is apparently the case for H⁺ form resin. Hydrogen gas generation in samples contacted with corrosion coupons far exceeds radiolytic hydrogen formation in the resin alone (Swyler, Dodge and Dayal, 1983). A correlation between the amount of hydrogen generated and corrosion coupon weight loss indicates that about 0.8 mole of H₂ is produced for every mole of Fe lost to corrosion (Figure 3.14).

For other resin forms, the corrosion rates are lower, and corrosion effects on radiolytic hydrogen generation are less obvious. Comparative hydrogen gas generation data on resin irradiated with and without corrosion coupons are given in Table 3.2.

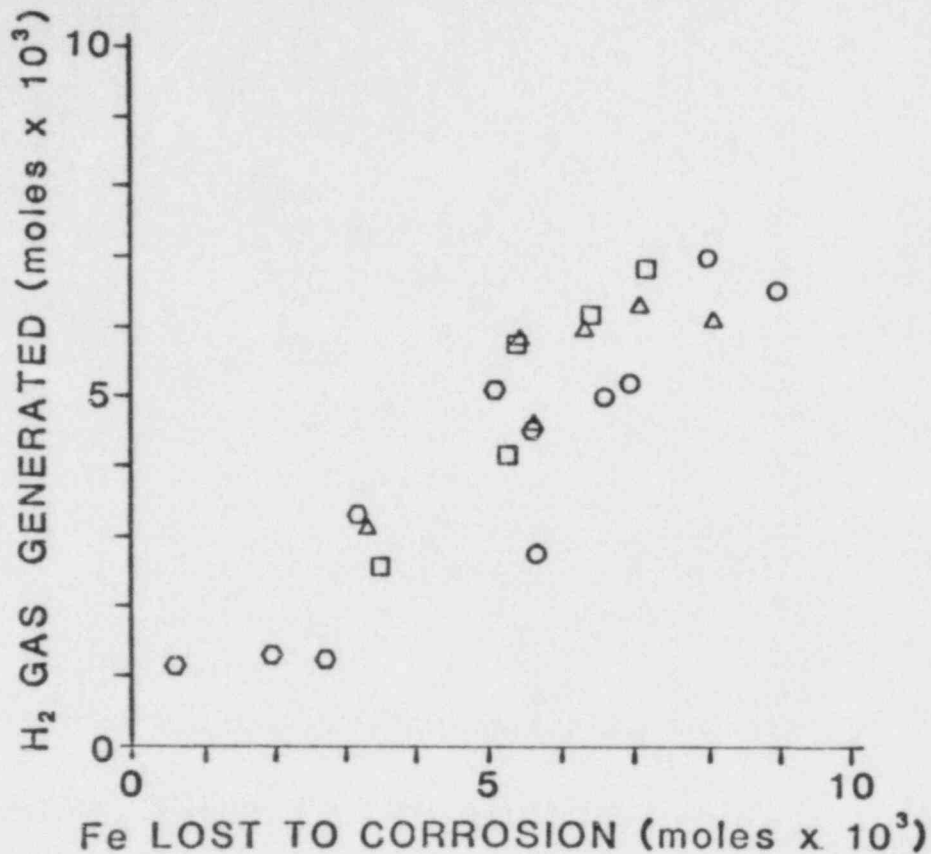


Figure 3.14 Hydrogen gas yields vs corrosion weight loss in mild steel coupon contacted with H⁺ form IRN-77 resin; radiation dose rates (rad/h): o = 1.7 x 10⁶; □ = 1 x 10⁵; Δ = 4 x 10⁴; ○ = unirradiated.

For resins other than H⁺ form there is no evidence that the weight loss in mild steel corrosion is quantitatively correlated with increased hydrogen generation. For the Na⁺ form resin, the net corrosion (molar) weight loss is significantly greater than the (molar) hydrogen evolution at lower radiation dose rates (4x10⁴ and 1x10⁵ rad/h). At 1.6x10⁶ rad/h there is one data point which suggests that hydrogen generation may be caused by corrosion. For the Cs⁺ form resin, there is also evidence that corrosion results in increased hydrogen generation. Again, however, all the corrosion weight loss (molar) is not accounted for by hydrogen gas generation.

Table 3.2
Radiolytic Hydrogen Yields, Hydrogen Uptake in Corrosion, and
Mild Steel Corrosion Weight Loss in Irradiated Resins

Resin Form	Moles Radiolytic H ₂		Fe weight loss (moles)	H ⁺ a Consumption (moles)
	With Coupon	Without Coupon		
IRN-77 Na ⁺ 4x10 ⁴ rad/h	--	--	2.5x10 ⁻⁴	~1 x10 ⁻⁶
	--	--	2.9x10 ⁻⁴	~3 x10 ⁻⁶
	--	--	4.0x10 ⁻⁴	5.7x10 ⁻⁶
	--	--	4.6x10 ⁻⁴	1.3x10 ⁻⁵
	--	--	4.1x10 ⁻⁴	1.4x10 ⁻⁵
	--	1.6x10 ⁻⁵	6.2x10 ⁻⁴	1.3x10 ⁻⁵
	4.6x10 ⁻⁵	5.9x10 ⁻⁵	1.7x10 ⁻³	--
	--	--	1.3x10 ⁻³	--
IRN-77 Na ⁺ 9.8x10 ⁴ rad/h	1.5x10 ⁻⁴	1.5x10 ⁻⁴	2.5x10 ⁻³	--
	1.8x10 ⁻⁴	2.1x10 ⁻⁴	2.5x10 ⁻³	--
	--	--	--	1.1x10 ⁻⁵
	--	--	3.1x10 ⁻⁴	1.0x10 ⁻⁵
	--	--	4.4x10 ⁻⁴	1.9x10 ⁻⁵
	--	--	8.1x10 ⁻⁴	2.9x10 ⁻⁵
	--	--	5.9x10 ⁻⁴	3.7x10 ⁻⁵
	--	5.0x10 ⁻⁵	8.8x10 ⁻⁴	--
IRN-77 Na ⁺ 1.6x10 ⁶ rad/h	--	--	1.4x10 ⁻³	--
	--	--	2.5x10 ⁻³	--
	--	--	3.4x10 ⁻³	--
	--	--	9.7x10 ⁻⁴	1.2x10 ⁻⁴
	--	--	1.3x10 ⁻³	1.3x10 ⁻⁴
	--	--	1.7x10 ⁻³	1.6x10 ⁻⁴
	--	--	2.2x10 ⁻³	1.8x10 ⁻⁴
1.6x10 ⁻³	3.5x10 ⁻³	2.4x10 ⁻³	2.1x10 ⁻⁴	
--	--	2.4x10 ⁻³	2.0x10 ⁻⁴	

Table 3.2 (cont.)
Radiolytic Hydrogen Yields, Hydrogen Uptake in Corrosion, and
Mild Steel Corrosion Weight Loss in Irradiated Resins

Resin Form	Moles Radiolytic H ₂		Fe weight loss (moles)	H ⁺ a Consumption (moles)
	With Coupon	Without Coupon		
IRN-77 Cs ⁺	--	--	9.3x10 ⁻⁴	3.0x10 ⁻⁴
1.6x10 ⁶ rad/h	5.4x10 ⁻⁴	1.2x10 ⁻³	1.4x10 ⁻⁴	3.0x10 ⁻⁵
	--	--	2.1x10 ⁻³	4.5x10 ⁻⁴
	--	--	1.9x10 ⁻³	5.7x10 ⁻⁴
	--	--	2.2x10 ⁻³	6 x10 ⁻⁴
	2.1x10 ⁻³	2.5x10 ⁻³	2.7x10 ⁻³	--
	2.2x10 ⁻³	2.6x10 ⁻³	2.5x10 ⁻³	--
IRN-150 HOH	3.6x10 ⁻⁴	3.4x10 ⁻⁴	3.1x10 ⁻⁴	--
1.6x10 ⁶ rad/h	--	1.0x10 ⁻³	3.5x10 ⁻⁴	2.8x10 ⁻⁵
	--	--	4.4x10 ⁻⁴	8.5x10 ⁻⁵
	--	--	8.0x10 ⁻⁴	1.4x10 ⁻⁴
	--	--	8.1x10 ⁻⁴	1.9x10 ⁻⁴
	3.4x10 ⁻³	2.4x10 ⁻³	8.8x10 ⁻⁴	2.7x10 ⁻⁴
	4.7x10 ⁻³	--	9.8x10 ⁻⁴	--
IRN-150 NaCl	2.9x10 ⁻⁴	2.7x10 ⁻⁴	1.4x10 ⁻⁴	9.1x10 ⁻⁶
1.6x10 ⁶ rad/h	--	--	2.0x10 ⁻⁴	5.6x10 ⁻⁵
	1.4x10 ⁻³	1.2x10 ⁻³	4.8x10 ⁻⁴	1.7x10 ⁻⁴
	--	--	5.8x10 ⁻⁴	3.1x10 ⁻⁴
	2.2x10 ⁻³	2.5x10 ⁻³	8.8x10 ⁻⁴	3.9x10 ⁻⁴
	2.5x10 ⁻³	2.7x10 ⁻³	1.2x10 ⁻³	2.0x10 ⁻⁴

^aHydrogen consumption was determined from the difference in supernatant pH for samples with and without corrosion coupons.

-- = Not measured.

We have estimated the amount of hydrogen ion which would have to be consumed in order to produce the supernate and free liquid pH elevation observed in samples contacted with corrosion coupons. This was done by subtracting $[H^+]$ values for samples without corrosion coupons from $[H^+]$ value for samples containing corrosion coupons. $[H^+]$ was simply determined from pH data for the free liquid or supernate samples. The concentration differences (in mol/l) were then multiplied by the liquid volumes to obtain molar H^+ consumption. Values obtained in this way are shown in the right column of Table 3.2. The calculation also assumes uniform depletion throughout the resin sample. Amounts of H^+ in the supernate over 2 g of resin were multiplied by 3, since the supernate was measured in only 2 g of the 6 g resin samples.

Under these assumptions, the molar values for H^+ consumption are consistently lower than the (molar) values for iron lost in corrosion. If, in fact, values for H^+ obtained in this way are valid, the corrosion is greater than would be expected on the basis of resin acidity neutralization alone. It is also possible that the pH changes do not accurately reflect the total hydrogen ion uptake in the simple manner assumed here; this will be considered further in Section 7.

3.5 Transport of Corrosive Species and Corrosive Products in Resin Beds

3.5.1 Chemical Analysis of Corrosion Products in Irradiated Resin Columns

Short-term column experiments were carried out to examine the distribution of corrosion products and acidic species in fully swollen cation resin contacted with corrosion coupons. The general arrangement of these column experiments has been described in Section 2. A typical experiment is shown in Figure 3.15.

Table 3.3 gives the results of a column experiment in which corrosive coupons were placed on top of 10 cm H^+ and Na^+ resin columns in glass and irradiated. The irradiations were carried out in vented tubes at 4×10^6 rad/h. Data are also given for irradiated control samples. Following irradiation resin samples were removed from different zones of the columns. Properties of the supernate formed by contacting the irradiated resins with deionized water in the ratio 2 g/10 mL were determined. The resins were then rinsed with H_2O and HNO_3 , and the amount of iron removed by each rinse was determined. Finally the resins were combusted and the residue analyzed to determine the amount of iron bound in the resin.

In the Na^+ form resin, irradiation again clearly enhances corrosion. Most of the corrosion product, as iron, is found in the top quarter of the bed, less than 2 cm from the corrosion coupon. Between fifteen and twenty percent of the total iron lost to corrosion, as indicated by coupon weight loss was found in the resin. The amount of iron on the sodium form resin is considerably lower than the amount of free sulfate produced. The sulfate data support the earlier observation that under the present conditions, radiolytic scission of the functional group was not significantly affected by mild steel corrosion products.

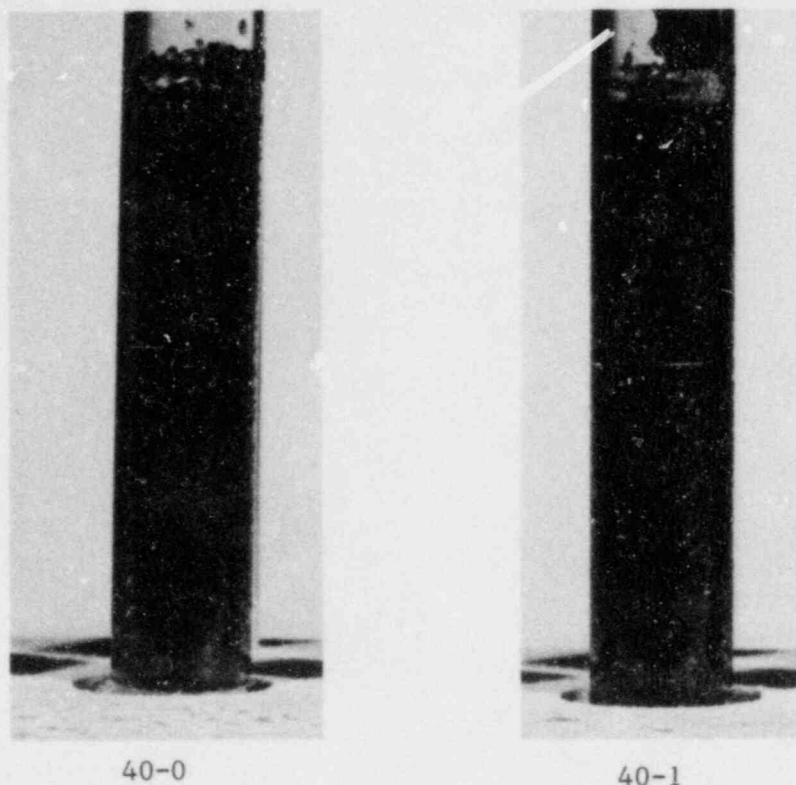


Figure 3.15 Irradiated IRN-77 Na⁺ form resin with (left) and without (right) corrosion coupons. Radiation dose = 10⁹ rad, time = 300 hours.

When comparison is possible, sulfate data for Na⁺ and H⁺ forms agree well both with each other, and with previous measurements on samples irradiated in sealed tubes (Swyler, Dodge and Dayal, 1983). This agreement further supports the observation that radiolytic attack of the functional group is not strongly dependent on resin pH or the amount of oxygen present.

pH values for the resin with corrosion coupons are greater than those for irradiated resins. Again acidic species are evidently taken up in the corrosion process. For the Na⁺ form resin the specific corrosion weight loss after 10 days in the irradiated columns was 27 mg/cm², corresponding to 5.8x10⁻⁴ total moles of Fe. The specific weight loss in the column experiments is greater than the value (~15 mg/cm²) which would be expected from data on corrosion experiments carried out in sealed vessels with a different coupon geometry (Figure 3.1).

For both the H⁺ and Na⁺ form resin, there is no indication of an extensive gradient in column acidity--the pH varies only slowly throughout the column. This might indicate either a reasonably uniform depletion of acidic species, or a localized depletion where the gradient is confined to a region that is small compared to the first two cm of the column. Finally it is worth noting that a large fraction of the iron in the irradiated resin was not removed in a H₂O rinse, but required a nitric acid rinse for removal. This indicates that the iron is either on the resins in an exchangeable form or that the iron is relatively insoluble.

-4-
Table 3.3
Distribution of Corrosion Products and Acidic Species in Irradiated Resin Columns

Resin Type	Radiation ^a Dose (Rad)	Column ^b Zone	Sample Wt(g)	Sample Moisture (%)	Supernatant ^c pH	% Content in Resin (Moles)					Material Loss From Coupon		
						SO ₄ in Supernatant (Moles/g resin)	H ₂ O ^d Rinse	HNO ₃ ^d Rinse	Bound ^e in Resin	Total Moles	Total Moles Fe	Mg/cm ²	% Fe in Resin
Na ⁺ with Coupon	10 ⁹	A	1.0	40	2.0	4.2x10 ⁻⁴	2.7x10 ⁻⁶	8.9x10 ⁻⁵	1.9x10 ⁻⁶	9.3x10 ⁻⁵	5.8x10 ⁻⁴	17	15
		B	1.3	43	1.9	4.9x10 ⁻⁴	--	--	2.8x10 ⁻⁶	2.8x10 ⁻⁶			
		C	0.8	42	1.8	5.3x10 ⁻⁴	--	--	--	--			
		D	1.5	44	1.8	4.6x10 ⁻⁴	--	--	--	--			
Na ⁺ with Coupon	0	A	1.2	41	5.3	1.1x10 ⁻⁶	--	5.4x10 ⁻⁶	1.2x10 ⁻⁵	1.7x10 ⁻⁵	8.8x10 ⁻⁵	4	10
		B	1.2	42	5.4	--	--	3.2x10 ⁻⁷	3.2x10 ⁻⁷				
		C	1.4	43	5.6	--	--	7.9x10 ⁻⁷	7.9x10 ⁻⁷				
		D	1.1	45	5.4	9.1x10 ⁻⁷	--	--	--	--			
Na ⁺	10 ⁹	A	1.8	40	1.7	5.5x10 ⁻⁴	--	--	--	--			
		B	1.5	41	1.7	5.0x10 ⁻⁴	--	--	--	--			
		C	0.9	43	1.7	4.4x10 ⁻⁴	--	--	--	--			
		D	0.8	44	1.7	5.1x10 ⁻⁴	--	--	--	--			
H ⁺ with Coupon	10 ⁹	A	1.2	57	1.2	5.1x10 ⁻⁴	4.2x10 ⁻⁵	2.5x10 ⁻⁴	3.9x10 ⁻⁶	2.9x10 ⁻⁴	8.2x10 ⁻⁴	39	36
		B	1.2	52	1.1	5.0x10 ⁻⁴	--	--	5.1x10 ⁻³	--			
		C	1.4	55	1.0	5.2x10 ⁻⁴	--	--	--	--			
		D	1.1	55	1.1	4.7x10 ⁻⁴	5.1x10 ⁻⁶	1.4x10 ⁻⁵	4.0x10 ⁻⁷	1.9x10 ⁻⁵			
H ⁺ with Coupon	0	A	1.3	47	2.8	1.7x10 ⁻⁶	--	7.9x10 ⁻⁴	1.9x10 ⁻⁴	9.0x10 ⁻⁴	1.6x10 ⁻³	74	63
		B	1.3	53	3.1	--	--	3.4x10 ⁻⁵	1.7x10 ⁻⁶	3.5x10 ⁻⁵			
		C	1.0	52	3.1	--	--	--	3.1x10 ⁻⁷	3.1x10 ⁻⁷			
		D	0.5	51	3.1	9.8x10 ⁻⁸	--	--	2.6x10 ⁻⁷	2.6x10 ⁻⁷			
H	10 ⁹	A	1.2	53	1.0	4.9x10 ⁻⁴	--	--	--	--			
		B	1.1	56	1.0	4.9x10 ⁻⁴	--	--	--	--			
		C	1.3	54	1.0	5.3x10 ⁻⁴	--	--	--	--			
		D	1.2	55	1.1	4.4x10 ⁻⁴	--	--	--	--			

^aDose Rate - 4x10⁶ rad/h. Samples irradiated in vented tubes, corrosion coupons at top of column.

^bA - Upper 1/4 (~2 cm) of column in contact with corrosion coupon.

B - Second 1/4 of column (~2 cm).

C - Third 1/4 of column (~2 cm).

D - Bottom 1/4 of column (~2 cm).

^cpH of supernatant formed by contacting deionized water with irradiated resin in the ratio 2 g resin: 10 ml D.I.W.

^dMoles Fe removed by rinsing resin with 100 mL of indicated solutions.

^eMoles Fe found in resin on combustion following H₂O and HNO₃ rinse.

Table 3.4 gives data for resins contacted with corrosion coupons in a reverse configuration--the corrosion coupon is at the bottom of the column. The height of the column was varied from 13 to 50 mm, to determine if corrosion rates were affected by the amount of resin present.

Table 3.4
Distribution of Corrosion Products in Irradiated Resin Columns of Different Height.^a

Resin Type	Column ^b Height	Radiation ^c Dose	Material Lost From Coupons		Resin Moisture After Contact (wt %)		
			Total Moles Fe	Total mg/cm ²	Bottom	Middle	Top
H ⁺	13	1x10 ⁸	--	--			
		5x10 ⁸	--	--			
		1x10 ⁹	8.4x10 ⁻⁴	40	36		58
	25	1x10 ⁸	--	--			
		5x10 ⁸	--	--			
		1x10 ⁹	7.2x10 ⁻⁴	35	36		
	50	1x10 ⁸	--	--			
		5x10 ⁸	--	--			
		1x10 ⁹	5.4x10 ⁻⁴	26	41	54	60
Na ⁺	13	1x10 ⁸	--	--			
		5x10 ⁸	--	--			
		1x10 ⁹	7.2x10 ⁻⁴	34	36		37
	25	1x10 ⁸	--	--			
		5x10 ⁸	--	--			
		1x10 ⁹	8.4x10 ⁻⁴	41	36	30	36
	50	1x10 ⁸	--	--			
		5x10 ⁸	--	--			
		1x10 ⁹	4.2x10 ⁻⁴	25	39		42

^aIrradiated 12.7 mm pyrex tubes with corrosion coupons at bottom of resin column.

^bHeight of column over coupon.

^cDose rate 4×10^6 rad/h.

Corrosion weight loss did not vary systematically with height of the resin column. Interestingly, for both resin types, corrosion in the shortest column (13 mm) was greater than corrosion in the longest column (50 mm). The total corrosion values are about the same for H⁺ and Na⁺ form resins and agree fairly well with data obtained earlier for coupons at the top of the resin columns (Table 3.3). Again, the corrosion weight loss in the Na⁺ form resin in these column experiments is significantly greater than that found in coupons contacted with resins and irradiated in sealed vessels. Overall, for both column experiments, there is no evidence that resins more than ~1.5 cm away from the coupon contribute significantly to the corrosion process.

3.5.2 Chemical Analysis of Corrosion Products in Resin/Sulfuric Acid Mixtures

In a separate series of measurements, mild steel corrosion in mixtures of resin and sulfuric acid was studied. The object was to determine how well corrosion in resins could be simulated by H_2SO_4 attack. Two grams of IRN-77 resin are contacted with 10-mL solutions of sulfuric acid of various strengths until a pH is obtained which is similar to that found in the supernate over irradiated resins. Next, the resin was either held immersed in solution or centrifuged to approximately 50% moisture content. Both immersed and centrifuged samples were then contacted with mild steel corrosion coupons.

Immersion simulates conditions which might occur if free liquid collects in a container. Immersion may in principle modify the transport of corrosive species within the resin bed, atmospheric oxygen scavenging and atmospheric effects on corrosion. Subsequently, the corrosion and other properties are observed as a function of contact time.

Immersion in resin-sulfuric acid solutions did not reproduce the type of corrosion on the weight loss observed with irradiated resins (Table 3.5). The corrosion was reasonably uniform.

Table 3.5
Weight Loss for Mild Steel Corrosion Coupon After 10-Day Contact
with Resin- H_2SO_4 Solutions

Sample	Resin Form	pH		Corrosion Coupon
		H_2SO_4	H_2SO_4 + Resin After 3 Days	Weight Loss (moles)
1	H ⁺	0.80	0.95	3.2×10^{-3}
2	"	1.08	1.23	2.8×10^{-3}
3	"	1.86	1.69	2.8×10^{-3}
4	"	2.56	2.40	2.5×10^{-3}
5	"	5.00	3.37	8.2×10^{-4}
1	a	0.80	0.98	4.3×10^{-4}
2	"	1.08	1.33	3.8×10^{-4}
3	"	1.86	2.33	2.0×10^{-4}
4	"	2.56	4.03	7.1×10^{-5}
5	"	5.00	5.02	--

Pitting corrosion of the type observed with irradiated IRN-77 resin can in fact be reproduced by "loading" unirradiated resins with sulfuric acid described above, i.e. by contacting the resin with sulfuric acid and then centrifuging the free liquid off. Several columns of Na⁺ and H⁺ form resin at different pH were prepared and contacted with corrosion coupon discs placed at

the top of the column. Results are shown in Table 3.6. Within the individual columns, the pH of the resin in the upper and lower halves does not differ substantially. In fact, the upper portion, which is in contact with the corrosion coupon, is generally somewhat more acidic. Since the effect of corrosion is to elevate the overall pH, the lack of a pronounced pH gradient within the tube suggests that, in the resin, transport processes are operative over a distance of at least several centimeters. This is in contrast to the results obtained with irradiated resins (Table 3.3). Also a much larger fraction of the iron corrosion product is found in the resin loaded with H_2SO_4 .

For an initial pH value of 3.3, the mild steel corrosion in the sulfuric acid loaded sodium form resin corresponds fairly well to that for the irradiated resin column after a 10 day contact time. However, the transport of acidic species and corrosion products is evidently somewhat different in irradiated and acid loaded resins.

Table 3.6
Distribution of Corrosion Products and Acidic Species in Resin Columns Loaded with H₂SO₄^a

Resin Type	Column Zone	Sample wt(g)	Supernatant pH ^a		Fe in Resin (moles)				Material Lost From Coupon		
			Initial	Final	H ₂ O ^d Rinse	HNO ₃ ^d Rinse	Bound ^e in Resin	Total Moles	Total Moles Fe	mg/cm ²	% Fe in Resin
Na ⁺ -1	Top	0.68	4.4	7.3	--	1.2x10 ⁻⁵	5.2x10 ⁻⁵	1.1x10 ⁻⁴			
	Bottom	0.84	"	8.2	--	1.1x10 ⁻⁶	2.7x10 ⁻⁷	6.6x10 ⁻⁵		5.1	61
Na ⁺ -2	T	1.0	3.3	6.2	--	2.9x10 ⁻⁵	7.8x10 ⁻⁵				
	B	1.1	"	6.4	--	5.1x10 ⁻⁷	1.7x10 ⁻⁷	1.1x10 ⁻⁴	1.9x10 ⁻⁴	8.9	59
Na ⁺ -3	T	1.0	3.0	5.1	--	1.7x10 ⁻⁴	2.0x10 ⁻⁴				
	B	0.75	"	5.3	--	3.7x10 ⁻⁵	9.0x10 ⁻⁶	4.2x10 ⁻⁴	8.0x10 ⁻⁵	40	51
Na ⁺ -4	T	1.2	1.9	4.2	1.6x10 ⁻⁶	3.8x10 ⁻⁴	3.2x10 ⁻⁴				
	B	0.84	"	4.0	2.7x10 ⁻⁷	2.7x10 ⁻⁴	3.2x10 ⁻⁵	9.8x10 ⁻⁴	1.4x10 ⁻³	65	70
Na ⁺ -5	T	0.72	6.0	7.2	--	7.8x10 ⁻⁶	5.4x10 ⁻⁵				
	B	1.1	"	8.3	--	1.7x10 ⁻⁷	1.0x10 ⁻⁷	6.9x10 ⁻⁵	8.5x10 ⁻⁵	4.1	80
H ⁺ -1	T	1.1	3.2	3.1	--	8.8x10 ⁻⁴	1.7x10 ⁻⁴				
	B	0.1	"	2.1	--	1.0x10 ⁻⁴	2.2x10 ⁻⁵	1.1x10 ⁻³	1.3x10 ⁻⁷	63	90
H ⁺ -2	T	1.2	3.0	2.9	--	8.5x10 ⁻⁴	1.1x10 ⁻⁴				
	B	0.7	"	3.5	--	1.1x10 ⁻⁴	2.4x10 ⁻⁵	1.2x10 ⁻³	1.4x10 ⁻³	68	77
H ⁺ -3	T	1.3	2.3	2.3	9.2x10 ⁻⁷	9.2x10 ⁻⁴	1.6x10 ⁻⁵				
	B	0.8	"	2.5	--	4.7x10 ⁻⁴	9.5x10 ⁻⁵	1.6x10 ⁻³	2.0x10 ⁻³	97	28
H ⁺ -4	T	1.1	1.4	1.9	2.0x10 ⁻⁶	8.1x10 ⁻⁴	2.0x10 ⁻⁵				
	B	0.9	"	2.4	--	5.9x10 ⁻⁴	9.2x10 ⁻⁵	1.7x10 ⁻³	2.5x10 ⁻³	122	65
H ⁺ -5	T	0.8	4.0	3.1	1.7x10 ⁻⁷	7.1x10 ⁻⁴	9.5x10 ⁻⁵				
	B	0.7	"	3.6	--	1.3x10 ⁻⁴	2.4x10 ⁻⁵	9.7x10 ⁻⁴	1.4x10 ⁻³	66	69

^aResins contacted with H₂SO₄ inducted and centrifuged to ~50% moisture. Samples contacted with coupons for 10 days, in vented tubes with corrosion coupons at top of column.

^bTop - upper half of columns (~1.5 cm) in contact with coupon.
Bottom - lower half of columns (~1. cm).

^cpH of supernate formed by contacting resin with deionized water.
in the ratio 2g resin: 10 ml D.I.W. Initial at start of experiment; final after 10 days contact time.

^dMoles removed by rinsing resin.

^eMoles Fe found in resin on combustion following rinse.

3.5.3 Spatial Extent of Resin Blackening Due to Mild Steel Corrosion

IRN-77 cation resin blackens due to the interaction with mild steel corrosion coupons. This blackening has been found to occur under the following conditions in the various experiments described in this report.

1. A slight blackening occurs nears the resin/coupon interface with unirradiated resin under oxic conditions. For H^+ form resin blackening also occurs for unirradiated resin stored in sealed vessels.
2. More intense blackening occurs for irradiated resin coupon columns; the blackened zone proceeds along the column as the irradiation progresses.
3. A similar blackened zone propagates in unirradiated resin columns which have been "loaded" with H_2SO_4 .
4. When IRN-77 resin is converted either to Fe^{+2} or Fe^{+3} form, the resin does not blacken. Irradiated Fe^{+2} or Fe^{+3} form resin, however, blackens markedly.

It has been mentioned by Egorov and Novikov (Egorov and Novikov, 1967) that when H^+ ions of irradiated cation resin are exchanged for Fe^{+3} ions, the resin turns black. This effect is said to be an indirect confirmation of the presence of carboxylic and phenolic groups in the irradiated resin, since sulfosalicylic acid, which contains these groups, is known to form a dark colored complex with Fe^{+3} ions. The sulfosalicylic acid would presumably result from radiolytic attack on the resin backbone.

In order to determine if this effect was involved in the darkening of resins contacted with corrosion coupons, irradiated and unirradiated H^+ form resins were contacted with Fe^{+2} and Fe^{+3} ions in solution to see if dark regions were formed.

Approximately 1 g portions of irradiated (3×10^8 rad) and unirradiated IRN-77 H^+ form resin were put into separate containers. Fe^{+2}/H_2SO_4 was added to one set of, Fe^{+3}/H_2SO_4 was added to another set of irradiated and unirradiated resins. After three days, the irradiated resin turned black in the presence of Fe^{+2} and Fe^{+3} solutions while the unirradiated resin showed no color change.

These results agree with the observations of Egorov and Novikov: there are certain sites in the irradiated resin which, when occupied by iron, turn the resin black. The sites involved are not ordinary exchange groups, since no blackening is produced when Fe^{+2} and Fe^{+3} are exchanged for H^+ in unirradiated resin. Blackening is observed, however, when Fe^{+2} and Fe^{+3} are added to irradiated resin.

The data suggest that the blackening is due to the presence of iron at a damaged site in the resin produced by irradiation. However, we were not

able to assign the resin blackening to sulfosalicylic acid. $\text{Fe}^{+2}/\text{H}_2\text{SO}_4$ and $\text{Fe}^{+3}/\text{H}_2\text{SO}_4$ solutions were added to sulfosalicylic acid (SSA) solution in the ratio 1:1. The Fe^{+2} and SSA remained clear while the Fe^{+3} solution with SSA turned pink. This experiment effectively rules out the formation of sulfosalicylic acid as the final form of the irradiated species, because the Fe^{+2} turned the irradiated resin black, but did not blacken the SSA solution. Ultraviolet adsorption spectra were also run with SSA. These did not agree at all with the spectra of the supernate above the resin.

A mild steel coupon placed in contact with an unirradiated resin will darken the resin, but a solution of Fe^{+2} or Fe^{+3} ions added to unirradiated resin has no effect. The corrosion induced darkening of an unirradiated resin evidently does not involve simple uptake of Fe^{+2} or Fe^{+3} . It is possible that darkening of unirradiated resin in a corrosion process involves iron located at damaged site in the resin. Unlike the case for irradiated resin, however, the damage would have to be produced in the corrosion process itself. Alternately the darkening could simply be due to partly soluble "rust." In either case the blacking would be much less extensive than that observed in irradiated resins for equal net corrosion. This is what is observed.

The resin blackening provides a measure of transport of corrosion products within the resin in the resin bed. In the column corrosion experiment, the travel of the blackened zone along this column was observed as a function of time. Migration of the blackened zone is plotted vs time for different experimental configurations in Figures 3.15 and 3.16.

For the irradiated resin columns with the corrosion coupon at the top, the blackened zone may extend up to 2 cm from the coupon after 10 days (this corresponds roughly to the extent of zone "A" referred to in Table 3.3). With the coupon at the top, the blackened zone showed an initial rapid growth, which slows down with time--after about 5 days the blackened zone did not grow noticeably. For the coupon on the bottom of the column the blackened zone is less extensive and grows more slowly--after 10 days the zone extended about 1 cm from the coupon.

For resin "loaded" with H_2SO_4 to simulate radiation damage, the blackened "corrosion" zone is not as large as in irradiated resins. The corrosion weight loss for the loaded resins, however, may be greater than in irradiated resins (compare the molar corrosion weight losses in Tables 3.4 and 3.6).

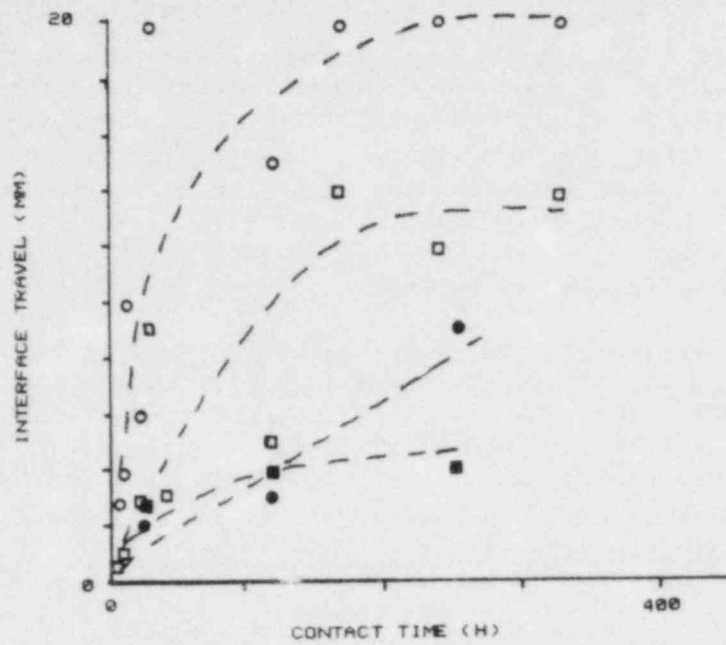


Figure 3.16 Growth of blackened resin zone in irradiated resin columns containing corrosion coupons. Open points - Column Height 50 mm, coupon at top of column. Solid Points - Column Height 50 mm, coupon at bottom of column. \circ = H^+ form resin, \square = Na^+ form resin. Radiation dose rate 3.6×10^6 rad/h.

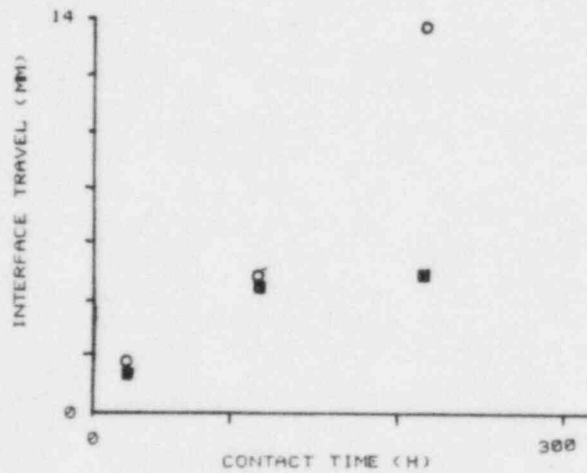


Figure 3.17 Growth of blackened resin zone in resin columns containing corrosion coupons and resins loaded with H_2SO_4 . Column height 25 mm. Open points-- H^+ form resin; initial pH values adjusted with H_2SO_4 to 1.4. Solid points-- Na^+ form resin, indicated pH values adjusted with H_2SO_4 to 1.9.

4. EFFECT OF AGING PROCESSES AND ENVIRONMENTAL CONDITIONS ON RESIN RADIOLYSIS

It has been recognized for some time that organic ion-exchange resins may undergo a time-dependent deterioration in the absence of irradiation (Armitage and Lyle, 1972). In polymers such as polyethylene, there is evidence that chemical degradation processes initiated by irradiation may continue for some time after the irradiation is terminated (Gillen and Clough, 1982).

The yield of resin radiolytic decomposition products may also depend on how the yields are measured. Rinsing irradiated resins, which is common practice, could produce different results from experiments in which irradiated resin is contacted with water in order to simulate waste intrusion conditions in a radwaste container. Finally, both the radiolytic attack on the resin and the post-irradiation degradation processes may be influenced by contact with external media such as air or water.

In this program, the majority of radiation damage measurements were carried out on supernatant solutions formed by contacting irradiated resin with deionized water. As mentioned earlier (Swyler, Dodge and Dayal, 1983), this approach, as opposed to rinsing, was adopted in order to measure yields under conditions more relevant to radwaste. In particular, it was decided to allow the resin to remain in contact with its own decomposition products. Also, most measurements were made on resins irradiated in sealed vessels--under these conditions the environment quickly became anoxic. However, to support development of recommended test procedures, experiments were also carried out to determine the possible effect of time-dependent and environmental factors on test results. In this section the results of such measurements are described.

4.1 Irradiation of IRN-77 Resin Under Vented (Oxic) Conditions

Radiolytic oxygen scavenging by irradiated resins has been described previously (Swyler, Dodge and Dayal, 1983). A remarkably efficient radiolytic reaction occurs in which both CO_2 and oxidized species in the resin are produced. Previous experiments emphasized the significance of this radiolytic process in preventing the formation of explosive conditions. The present experiments were carried out to examine the effect of the radiolytic oxidation on resin degradation.

Samples (6 g) of fully-swollen IRN-77 resins in H^+ and Na^+ forms were placed in Pyrex tubes of the same dimension as those used previously under a sealed condition. Once the tubes were loaded, the openings were necked down to form apertures ~ 1 mm in diameter. The samples were then irradiated at a dose rate of 1.5×10^6 rad/h. The purpose of the small aperture was to prevent excessive dehydration of the resins during irradiation, while allowing for interaction of the resins and atmospheric oxygen.

Following irradiation, overall weight change was determined by weighing the sample tubes. The resins were then contacted with deionized water in the ratio 2 g/10 mL. The pH and sulfate content of the supernate were then determined. For this experiment sulfate concentrations were measured by the colorimetric (Methyl-Thymol Blue) technique. Results are given in Table 4.1.

Table 4.1

Acidity, Soluble Sulfate and Weight Change
For IRN-77 Resin Irradiated Under Vented Conditions

Sample Type	Irradiation Time (h)	pH ^a	[SO ₄ ⁻] ^b	Sample Weight Change (%) ^c
Na+	168 ^d	5.9	N.M. ^e	0
	504 ^d	5.7	N.M.	-0.3
	1008 ^d	5.8	N.M.	-0.3
	168	2.7	2.1 x 10 ⁻⁴	-0.3
	336	2.2	4.4 x 10 ⁻⁴	0
	504	2.3	6.7 x 10 ⁻⁴	-0.7
	672	1.9	6.4 x 10 ⁻⁴	+0.7
	840	1.8	7.5 x 10 ⁻⁴	-0.3
	1008	1.6	1.0 x 10 ⁻³	-0.3
	H+	168 ^d	3.1	N.M.
504 ^d		3.6	N.M.	-0.3
1008 ^d		3.3	N.M.	-0.7
168		1.3	2.6 x 10 ⁻⁴	+2.0
336		1.2	4.9 x 10 ⁻⁴	+0.7
504		1.2	6.8 x 10 ⁻⁴	+3.0
672		0.9	8.3 x 10 ⁻⁴	+1.0
840		0.9	1.1 x 10 ⁻³	+2.0
1008		0.9	1.5 x 10 ⁻³	+1.0

^aTwo grams of resin in 10 mL deionized water.

^bTotal amount (moles) in solution, measured by the MTB method.

^cThe minimum detectable weight change is ~0.3%.

^dUnirradiated control samples, held for times indicated.

^eN.M. = not measured.

For unirradiated samples neither pH nor resin weight were significantly affected by holding the samples for up to six weeks in vented tubes. A slight weight loss (<1%) may reflect a decrease in moisture content. For irradiated samples, the principal observations are as follows:

1. Sulfate yields are fairly close to those measured previously (Swyler, Dodge and Dayal) for samples irradiated in sealed tubes. Oxidation apparently does not play a significant role in radiolytic scission of the functional group.
2. The pH of the supernate is significantly lower than that measured for samples irradiated in a closed system. The pH data in Table 3.2 represent values for fresh solutions (i.e. ~10 h after contact). It is anticipated that, as the solutions age, pH values may decrease further.
3. The H⁺ resin shows an increase in weight upon irradiation. The weight change is less systematic for Na⁺ form. An oxidation of 3% of the carbon atoms (as carboxyl groups) would produce an increase in weight of approximately 1%. For the H⁺ form, increases in weight of this order are observed, neglecting any weight loss as CO₂.

The observations above suggest that extensive attack on the resin backbone has taken place during irradiation under vented conditions. Consequently, the additional acidity observed may be related to soluble organic acids (e.g. benzylic sulfonic acids) produced in the scission of the backbone.

There is also visual evidence for radiation induced agglomeration, involving attack on the resin backbone. Figure 4.1(a) shows IRN-77 Na⁺ form resin irradiated to a dose of 1.2×10^9 rad in a sealed environment. Figure 4.1(b) shows resin irradiated to a similar dose under vented conditions.

The sample irradiated under vented conditions is partly congealed with the beads tending to stick together. There is no evidence of this in samples irradiated in a sealed environment. When the sample in Figure 4.1(b) was heated to 100°C for a moisture content determination, the sample blackened almost completely and fused into a crumbly solid. Thermally induced reactions in polymers following irradiation in an oxygen environment have been attributed to chain reactions initiated by the decomposition of hydroperoxides in the sample (c.f., Gillen and Clough, 1981).

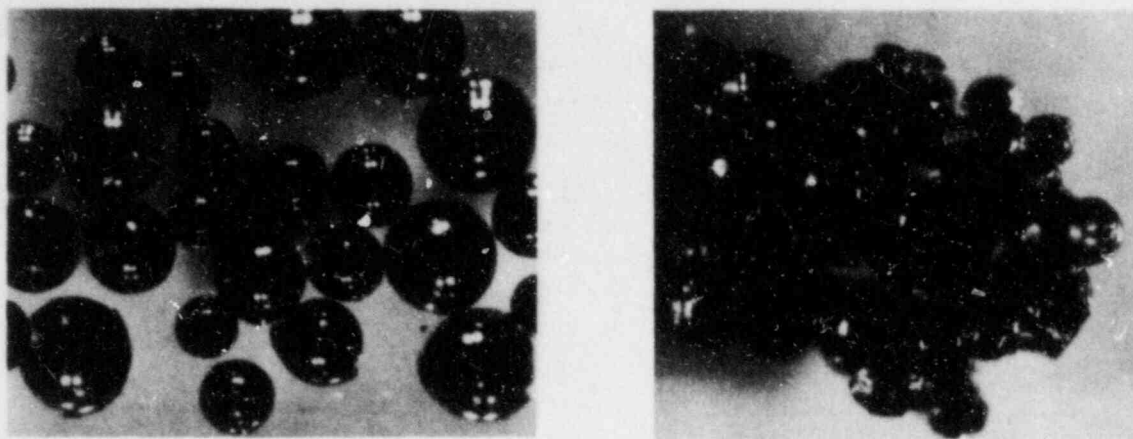


Figure 4.1 IRN-77 Na⁺ form resin irradiated to 1.2×10^9 rad under (a) sealed and (b) vented conditions.

4.2 Long-Term Irradiation Studies

Long-term irradiations on H⁺ and Na⁺ form resins at low dose rates have been completed. A major objective of these measurements, which have gone on for more than one year, is to examine the radiation dose rate dependence of the radiolytic degradation process in greater detail.

Figure 4.2 shows pH data and Figure 4.3 shows sulfate data for H⁺ and Na⁺ form IRN-77 resin which includes the long term measurements at 3×10^4 rad/h. In general, for the same total dose region, data at 3×10^4 rad/h and 1.6×10^6 rad/h overlap fairly well--no gross disparities exist. We conclude that, over the present dose and dose rate range, and for irradiation in a closed environment, radiolytic attack of the functional group is not sensitive to radiation dose rate.

Figure 4.4 gives hydrogen generation at different radiation dose rates and includes data for the long-term samples. H⁺ and Na⁺ form data at different dose rates fall roughly on the same curve. There is no gross departure from linearity which would indicate a pronounced dose rate effect on G-values.

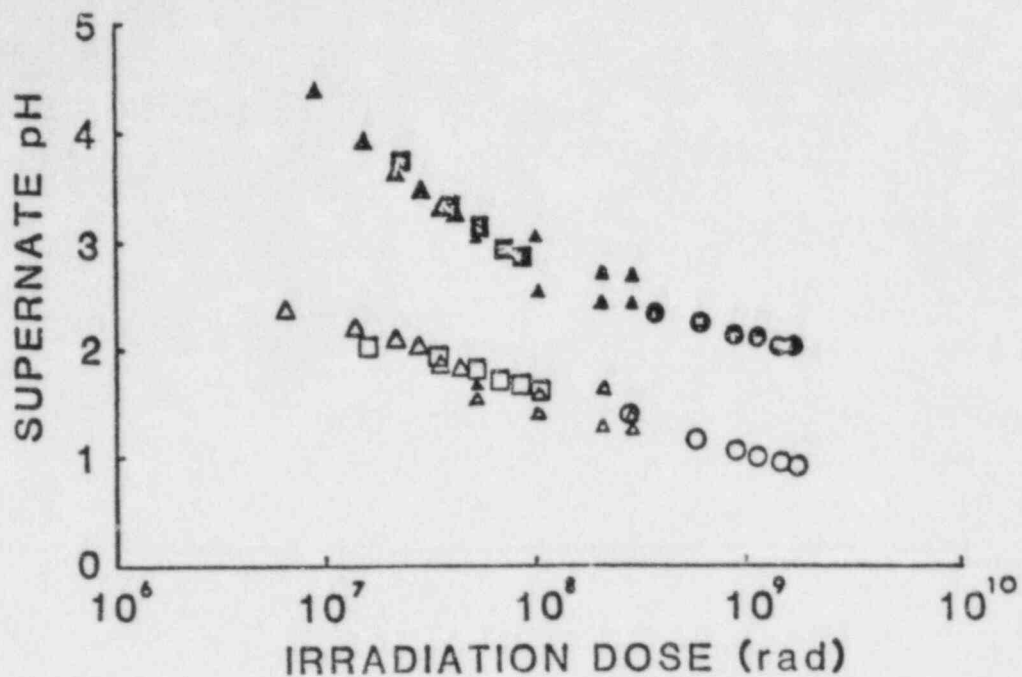


Figure 4.2 Supernatant pH vs irradiation dose in IRN-77 resin. Open points, H^+ form resin; solid points, Na^+ form resin; dose rate (rad/h) $\circ = 1.7 \times 10^6$; $\square = 1 \times 10^5 - 8 \times 10^4$; $\Delta = 4 \times 10^4 - 3.5 \times 10^4$.

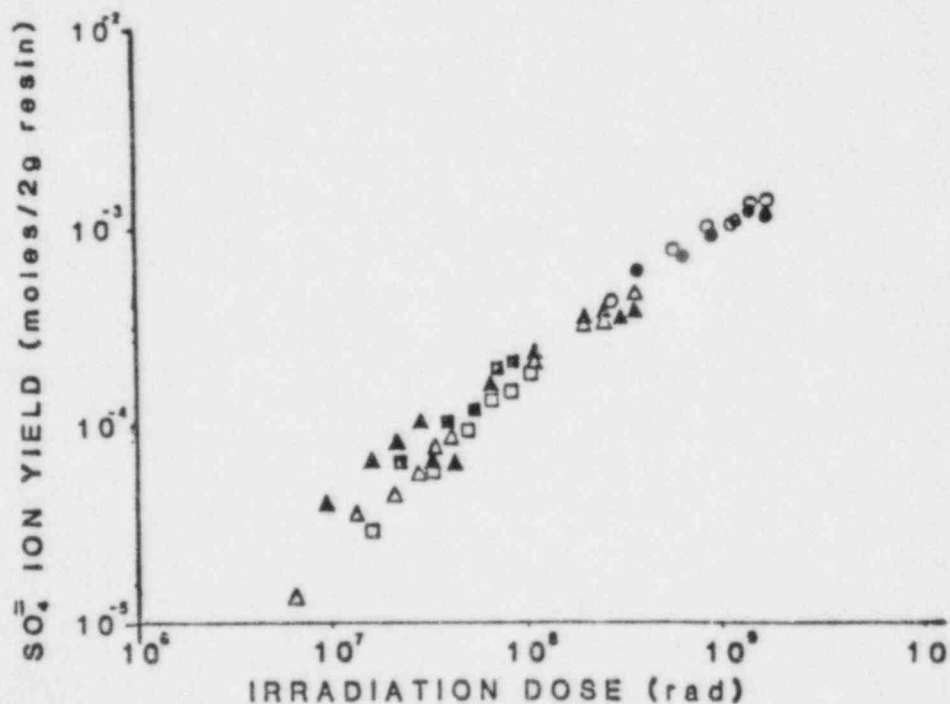


Figure 4.3 Supernatant sulfate yields vs irradiation dose in IRN-77 resin. Open points, H^+ form resin; solid points, Na^+ form resin; dose rate (rad/h) $\circ - 1.7 \times 10^6$; $\square = 1 \times 10^5 - 8 \times 10^4$; $\Delta = 4 \times 10^4 - 3.5 \times 10^4$.

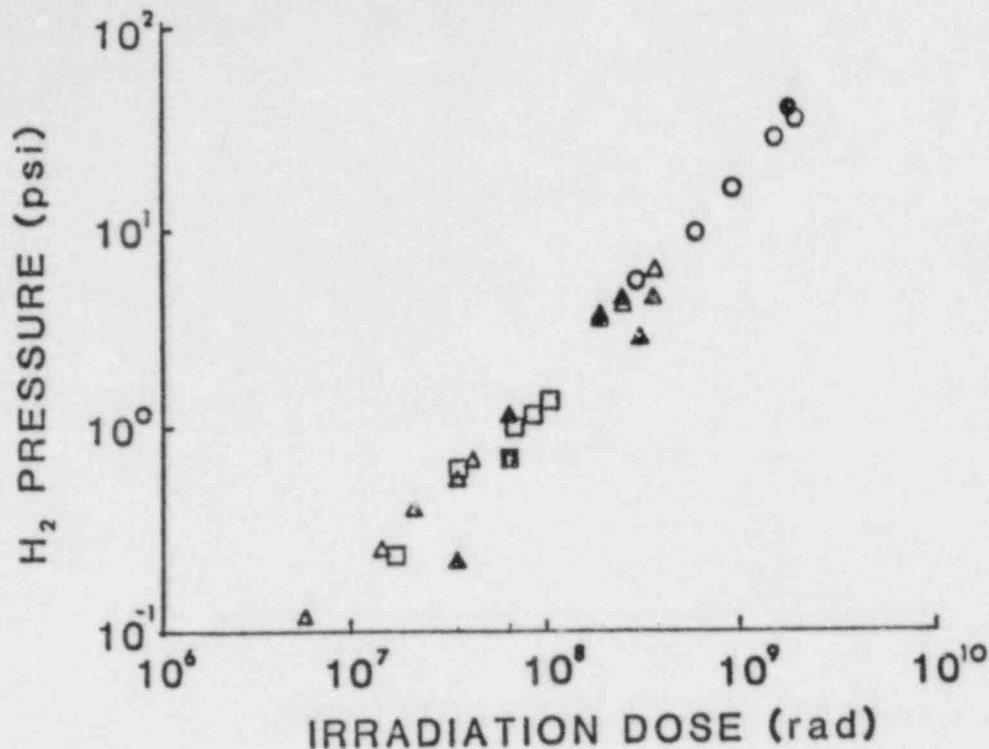


Figure 4.4 Radiolytic hydrogen gas generation in H^+ form (open points) and Na^+ form (solid points) IRN-77 resin; Radiation dose rate (rad/h) $\circ = 1.7 \times 10^6$; $\square = 1 \times 10^5 - 8 \times 10^4$; $\triangle = 4 \times 10^4 - 3.5 \times 10^4$.

Two specific features of the long-term data in Figures 4.2 and 4.3 are of particular interest from the viewpoint of aging effects. First, the long-term supernate pH data for both resin forms showed a decrease with increasing storage time. The resin-solution storage times varied from several months for the samples irradiated to doses below 10^8 rad to ~ 1 month for the sample with the greatest irradiation dose. Some of the pH decrease in the samples stored for long times can be attributed to liquid loss during storage.

For the sulfate data, a second feature is evident. In two cases, pairs of sulfate data points for a dose rate of 3.4×10^4 rad/h lie clearly below the general trend. These are the points at $\sim 5 \times 10^7$ rad and $\sim 5 \times 10^8$ rad. The values are lower by about a factor of 1.5 to 2. In each case, these points represent the ends of irradiation intervals and the resin or resin-DIW mixtures were not aged as long as those for lower total doses. For example, the difference in aging time for sodium form data near 10^8 rad and the data near 5×10^8 rad was approximately 8 months. This is the first suggestion we have seen for either a long-term (>1 month) increase in sulfate levels with time. This could also represent an effect in which sulfate release is retarded at high supernate concentrations. Concentration effects on sulfate release are considered further in Section 4.3. For the present, we simply point out that for different batches of Na^+ and H^+ form resin, irradiated at dose rates which differ by a factor of ~ 50 , supernatant sulfate levels at $\sim 3 \times 10^8$ rad agree to within a factor of 2 or less.

4.3 Aging Studies on Irradiated Resins and Resin-Water Solutions

The release rate of radiolytic resin decomposition products in aqueous solution may be limited by transport processes, possibly including an attractive (binding) interaction between the resin and the decomposition products. Such effects are common in leaching studies on radioactive waste forms and in studies of radionuclide transport through soils. Alternatively, the resin decomposition process may continue after the irradiation is terminated. Either of these mechanisms may produce time-dependent changes in the composition of solutions in contact with irradiated resins. General mechanisms which produce a time-dependent evolution of irradiated resin/solution properties may be termed "aging" processes. An extensive series of specific aging studies was not carried out. However, a number of experimental results were obtained in this program which can be applied to an assessment of the significance of aging effects on results and yields.

Tables 4.2 and 4.3 give results of supernatant pH measurements for solutions of two grams of irradiated cation resin in 10 mL of deionized water at different times after irradiation. The irradiations were carried out in sealed vessels and resin/water mixtures were stored in the dark in 25 mL capped polyethylene vials for the times indicated.

Table 4.2
Aging Effects on the Supernatant pH of Irradiated Resin/Water Solutions.

Cation Resin Form	Irradiation Dose Rate (rad/h)	Resin Irradiation Time (weeks)	Supernatant pH ^a				
			1 day ^b	1 week ^c	16 weeks ^b	30 weeks ^b	
H ⁺	4 x 10 ⁴	2	2.6	2.1	2.0		
		4	2.5	2.0	1.9		
		5	2.0	1.9	1.8		
	1 x 10 ⁵	2	2.5	1.9	1.8		
		4	2.1	1.7	1.8		
		5	2.1	1.7	1.6		
	1.6 x 10 ⁶	1	1.7	1.4	1.3		
		2	1.6	1.1	1.1		
		5	1.2	0.9	0.9		
	Na ⁺	4 x 10 ⁴	1.4	4.5	4.4		4.0
			3.4	3.9	3.7		3.3
			5.4	3.9	3.3		3.1
		1 x 10 ⁵	1.4	4.1	3.7		3.5
			3.4	3.5	3.1		2.8
			5.4	3.5	2.9		2.8
1.6 x 10 ⁶		2.4	2.6	2.3		2.2	
		3.4	2.4	2.1		2.1	
		4.4	2.3	2.1		1.9	

^aSupernatant over 2 g of irradiated resin in 10 mL deionized water.

^bMeasured in the same sample, held for times indicated following preparation.

^cMeasured in different samples of the same resin batch as (b), held for time indicated following preparation.

Table 4.3
Aging Effects on the Supernatant pH of Irradiated Resin Water
Solutions-Resins Contacted with Corrosion Coupons During Irradiation

Cation Resin Form	Irradiation Dose Rate (rad/h)	Resin Irradiation Time (weeks)	Supernatant pH ^a				
			1 day ^b	1 week ^c	30 weeks ^b	37 weeks ^b	
H ⁺	4 x 10 ⁴	2	3.1	2.4		2.4	
	4 x 10 ⁴	4	3.6	2.4		2.5	
	1 x 10 ⁵	2	2.6	2.2		2.3	
	1 x 10 ⁵	4	2.7	2.6		2.5	
	1.6 x 10 ⁶	2	2.6	2.2		2.1	
	1.6 x 10 ⁶	4	2.7	2.2		2.1	
	Na ⁺	4 x 10 ⁴	1	6.6	5.1	4.5	
		4 x 10 ⁴	3	6.0	4.5	4.4	
4 x 10 ⁴		5	4.6	4.2	4.2		
1 x 10 ⁵		1	6.9	4.6	4.4		
1 x 10 ⁵		3	4.3	4.2	4.0		
1 x 10 ⁵		5	3.9	4.0	3.9		
1 x 10 ⁶		2	3.6	3.1	2.9		
1 x 10 ⁶		3	3.8	2.9	2.4		
1 x 10 ⁶		4	3.8	2.8	2.7		

^aSupernate over 2 g of irradiated resin in 10 mL deionized water.

^bMeasured in the same sample, held for times indicated following preparation.

^cMeasured in different samples of same resin batch as (b) held for time indicated following preparation.

For resin-liquid contact times greater than about one week, the supernatant pH remained sensibly constant in these measurements. During the first week of contact, the pH might decrease by as much as 1 unit for the sodium form resin, although a decrease of ~0.5 unit is more typical.

In a second experiment, aged irradiated resin/water solutions were diluted tenfold with deionized water and the pH remeasured. Results are shown in Table 4.4. As expected, dilution results in an increase in pH. However, in an acidic solution a tenfold dilution should produce an increase of one pH unit. Since the observed increase is only 0.6 pH units, we attribute this discrepancy to the presence of other species that appear to contribute acidity and hence depress the expected pH increase upon dilution in the resultant solution.

Sulfate data measured in the supernate over irradiated resins for various aging correlations and resin-water ratios are shown in Tables 4.5, 4.6 and 4.7.

Over periods of several months there is no evidence for a systematic variation of radiolytic sulfate yields with time. This holds both for irradiation in sealed and vented systems, under different moisture conditions. Further, the dilution data do not indicate a strong dependence of sulfate yield on resin to water ratio. If anything, yields measured at higher dilutions appear to be slightly lower than those obtained from more concentrated solutions.

Table 4.4

Aging and Dilution Effects on the Aqueous Supernate pH
on Irradiated IRN-77 Resins

Sample	Dose Rate (rad/h)	Irradia- tion Time (wks)	Aging Time (wks)	Aged ^a pH	Aged pH After 10:1 Dilution ^b	
					12 h	96 h
H ⁺ resin with coupon	0	6	18	2.7	3.6	3.7
	4x10 ⁴	6	18	2.7	3.5	3.6
	1x10 ⁵	6	18	2.7	3.4	3.4
	1.6x10 ⁶	6	18	2.3	2.9	2.9
Na ⁺ resin with coupon	0	6	11	4.8	5.3	5.8
	4x10 ⁴	6	11	4.3	4.8	5.2
	1x10 ⁵	6	11	3.9	4.7	5.0
	1.6x10 ⁶	6	11	2.9	3.5	3.5
Na ⁺ resin	0	6.4	11	4.5	5.0	5.1
	4x10 ⁴	6.4	11	3.2	3.8	4.2
	1x10 ⁵	6.4	11	2.9	3.6	3.8
	1.6x10 ⁶	6.4	11	2.2	2.8	2.8

^aDilution = 2 g resin + 10 mL DIW.

^bDilution = 2 g resin + 110 mL DIW.

Table 4.5

Aging and Dilution Effects on the Sulfate Yield in the Supernate Over Irradiated Cation Resin.

Cation Resin Form	Irradiation ^a Dose Rate (rad/h)	Resin Irradiation Time (Weeks)	Supernatant SO ₄ Yield (Moles/2 g resin)		
			Sample 1	Sample 2	Sample 3
H ⁺ with coupon	0	5	5.7 x 10 ⁻⁶	7.3 x 10 ⁻⁶	5.9 x 10 ⁻⁶
	4 x 10 ⁴	5	3.3 x 10 ⁻⁵	2.7 x 10 ⁻⁵	2.6 x 10 ⁻⁵
	1 x 10 ⁵	5	6.9 x 10 ⁻⁵	6.7 x 10 ⁻⁵	4.9 x 10 ⁻⁵
	1.6 x 10 ⁶	5	7.7 x 10 ⁻⁴	6.7 x 10 ⁻⁴	5.9 x 10 ⁻⁴
Na ⁺ with coupon	1.6 x 10 ⁶	1	6.5 x 10 ⁻⁴	6.7 x 10 ⁻⁴	4.0 x 10 ⁻⁴
	1.6 x 10 ⁶	5	2.0 x 10 ⁻³	3.4 x 10 ⁻³	1.5 x 10 ⁻³
Na ⁺	1.6 x 10 ⁶	1.4	6.1 x 10 ⁻⁴	6.4 x 10 ⁻⁴	4.8 x 10 ⁻⁴
	1.6 x 10 ⁶	5.4	1.2 x 10 ⁻³	1.0 x 10 ⁻³	9.9 x 10 ⁻³

Sample 1. Irradiated resin stored 40-80 days; 2 g resin/10 mL water mixture aged 8-40 days.

Sample 2. Freshly irradiated resin; 2 g resin/10 mL water mixture aged 90 days-130 days.

Sample 3. Same as 2, diluted to 2 g resin/100 mL deionized water.

^aIrradiation carried out in sealed vessels.

Table 4.6
Dilution Effects on the Sulfate Yield in the Supernate Over Irradiated Cation Resins of Different Moisture Content.

Cation Resin Form	Resin Moisture Content (%)	Irradiation ^a Dose (rad)	Supernatant SO ₄ Yield (Moles/2g resin)	
			Sample 1	Sample 2
H ⁺	14	3 x 10 ⁸	1.6 x 10 ⁻³	1.1 x 10 ⁻³
Na ⁺	13	3 x 10 ⁸	5.1 x 10 ⁻⁴	5.1 x 10 ⁻⁴
Na ⁺	25	3 x 10 ⁸	4.7 x 10 ⁻⁴	4.7 x 10 ⁻⁴

Sample 1. 2 g irradiated resins in 10 mL deionized water, aged ~3 months.

Sample 2. Sample 1 aged an additional 4 months then diluted to 2 g resin/100 mL deionized water.

^aIrradiation carried out in vented vessels at 3.5 x 10⁶ rad/h.

Table 4.7
Aging Effects on the Sulfate Yield in the Supernate Over Irradiated Cation Resin.

Cation Resin Form	Irradiation ^a Dose Rate (rad/h)	Resin Irradiation Time (weeks)	Supernatant SO ₄ Yield (Moles/2g resin)	
			Sample 1	Sample 2
Na ⁺ with coupon	4 x 10 ⁴	2	5.8 x 10 ⁻⁵	3.0 x 10 ⁻⁵
	4 x 10 ⁴	4	1.1 x 10 ⁻⁴	1.2 x 10 ⁻⁴
	1 x 10 ⁵	4	2.0 x 10 ⁻⁴	1.8 x 10 ⁻⁴
Na ⁺	4 x 10 ⁴	2.4	6.8 x 10 ⁻⁵	7.3 x 10 ⁻⁵
	1 x 10 ⁵	1.4	6.6 x 10 ⁻⁵	7.6 x 10 ⁻⁵
	1 x 10 ⁵	4.4	2.0 x 10 ⁻⁴	1.9 x 10 ⁻⁴

Sample 1. 2 g irradiated resin in 10 mL deionized water, aged 5 weeks before measurement.

Sample 2. 2 g irradiated resins in 10 mL deionized water aged ~1 year before measurement.

^aIrradiation carried out in sealed vessels.

A comparison of pH and sulfate yields obtained by static leaching and by rinsing is given in Table 4.8. The yields obtained by rinsing the irradiated resins are generally somewhat lower than those found for static leaching in more concentrated solutions. The disparity is more pronounced at higher sulfate concentrations. Possible mechanisms accounting for this effect will be discussed in Section 7. Here, the important point is that there is no evidence that radiolytic sulfate yields measured by static leaching at the present resin to water ratio (2 g resin/10 mL deionized water) are suppressed by concentration effects at high irradiation doses.

Table 4.8
Comparison of Sulfate Yields in Resin Supernates and Rinses

Cation Resin Form	Irradiation Dose Rate (rad/h)	Irradiation Time (Weeks)	Supernate ^a		Rinse ^b	
			pH	SO ₄ ²⁻ yield ^c	pH	SO ₄ ²⁻ yield ^c
H ⁺	4 x 10 ⁴	2	2.0	3.5 x 10 ⁻⁵	2.7	
	4 x 10 ⁴	5	1.8	7.7 x 10 ⁻⁵	2.7	5.6 x 10 ⁻⁵
	1 x 10 ⁵	2	1.8	5.9 x 10 ⁻⁵	2.7	4.6 x 10 ⁻⁵
	1 x 10 ⁵	4	1.8	1.4 x 10 ⁻⁴	2.6	8.6 x 10 ⁻⁵
	1 x 10 ⁵	5	1.6	1.5 x 10 ⁻⁴	2.6	8.8 x 10 ⁻⁵
	1.6 x 10 ⁶	1	1.3	4.3 x 10 ⁻⁴	2.2	2.5 x 10 ⁻⁴
	1.6 x 10 ⁶	2	1.1	7.8 x 10 ⁻⁴	2.0	5.4 x 10 ⁻⁴
	1.6 x 10 ⁶	5	0.9	1.3 x 10 ⁻³	1.8	6.4 x 10 ⁻⁴
Na ⁺	4 x 10 ⁴	2.4	d	6.8 x 10 ⁻⁵	d	4.2 x 10 ⁻⁵
	4 x 10 ⁴	5.4	3.1	6.6 x 10 ⁻⁵	4.5	9.1 x 10 ⁻⁵
	1 x 10 ⁵	1.4	3.5	6.6 x 10 ⁻⁵	3.1	8.5 x 10 ⁻⁵
	1 x 10 ⁵	3.4	2.8	1.3 x 10 ⁻⁴	4.0	1.0 x 10 ⁻⁴
	1 x 10 ⁵	5.4	2.8	2.2 x 10 ⁻⁴	3.7	1.1 x 10 ⁻⁴
	1.6 x 10 ⁶	2.4	2.2	7.2 x 10 ⁻⁴	2.9	6.2 x 10 ⁻⁴
	1.6 x 10 ⁶	3.4	2.1	9.2 x 10 ⁻⁴	2.9	5.8 x 10 ⁻⁴
	1.6 x 10 ⁶	4.4	1.9	1.1 x 10 ⁻³	2.7	6.3 x 10 ⁻⁴
1.6 x 10 ⁶	5.4	d	1.3 x 10 ⁻³	d	9.0 x 10 ⁻⁴	

^aSupernate--Measured in supernate of 10 mL deionized water over 2 g irradiated resin.
^bRinse--Measured in the liquid obtained by rinsing the resin/water solutions with 90 mL deionized water.
^cSO₄²⁻ yield--moles SO₄²⁻ per 2 g resin
^dSupernate decanted before rinse and measured separately.

Finally, Table 4.9 gives aging effects on the supernate formed by contacting 10 mL of deionized water with 2g of unirradiated resin. Prior to contacting with deionized water, the resin had been held in contact with mild steel coupons for the times irradiated in the table.

The data show a gradual release of sulfate as a function of holding time, independent of irradiation. This is probably promoted by the corrosion process. The total amount released ($<2 \times 10^{-5}$ moles/2 g) is small compared to the amount typically observed for unirradiation dose of 10⁷ rad. For the largest values of sulfate release, the change in supernate [H⁺] with aging was about twice the change in [SO₄²⁻], consistent with the formation of H₂SO₄ in the aging process.

Table 4.9
Aging Effects on the pH and Sulfate Ion Content
of Aqueous Supernate of IRN-77 H⁺ Resin^a

Resin Holding Time (Weeks)	Fresh Supernate		Supernate Aging Time (Weeks)	Aged Supernate		$\Delta\text{SO}_4^{\equiv}$ ΔH^+
	pH	SO_4^{\equiv} (moles)		pH	SO_4^{\equiv} (moles)	
1	3.68	4.1×10^{-7}	6	2.73	6.8×10^{-7}	.016
2	2.91	3.4×10^{-6}	6	2.66	6.7×10^{-6}	.29
3	3.16	1.7×10^{-6}	6	2.90	3.2×10^{-6}	.27
4	2.84	3.7×10^{-6}	6	2.67	6.8×10^{-6}	.45
5	2.79	5.4×10^{-6}	6	2.63	9.3×10^{-6}	.54
6	2.60	1.0×10^{-5}	6	2.40	1.8×10^{-5}	.57

^aUnirradiated control samples contacted with mild steel corrosion coupons and held in sealed Pyrex vessel.

5. ELECTRON IRRADIATION EXPERIMENTS

Data on pH and gas yields are used to compare external electron vs gamma irradiation in simulating self-irradiation of heavily loaded dewatered resin wastes. pH data obtained for electron irradiated IRN-77 resins vs calculated absorbed dose are shown in Table 5.1. These are the entries denoted by (e^-). The table indicates that the pH values are in good agreement with those obtained following gamma irradiation. In Figure 5.1, a curve of pressure vs irradiation time is shown for IRN-77 resin electron irradiated in a sealed cell at 40°C. The dose rate is approximately 10^8 rad/h. The initial pressure rise is due to heating of the sample cell from 25 to 40°C; the subsequent pressure decreases indicated reflect gas uptake. For longer times, the pressure increases linearly with irradiation dose until the beam is interrupted. When the beam is restored, the pressure buildup proceeds as before.

When the beam current (proportional to radiation dose rate) is reduced to half its value, the rate of gas generation (as measured by the curve slope) is also decreased by a factor of two. Since no changes (other than thermal effects) are produced when the beam is interrupted, and the gas generation rate appears to vary linearly with dose rate, these results suggest that the net amount of gas generated by a given irradiation dose will be independent of dose rate.

In the present measurement, under electron irradiation at approximately 10^8 rad/h, we estimate a G value for gas formation of 0.3, where G is the number of molecules produced by an energy deposition of 100 eV. This value is generally commensurate with other determinations under gamma-irradiations at approximately 10^6 rad/h. Thus far, the present results, based strictly on net gas and pH "yields," do not provide any evidence either for inequivalence of electrons and gamma rays (on a per unit dose basis) or for significant radiation dose rate effects.

Table 5.1
Hydrogen Ion Concentration (as pH) of Water in Contact With
Irradiated Ion Exchange Resins

Dose (rad)	pH ^a			
	C-66%	C-66% (Na ⁺) ^b	IRN-77 (H ⁺)	IRN-77(Na ⁺)
0	4.4	7.0	3.5	6.8
10 ⁷ (Y)	2.6	---	2.5	4.7
1.25 x 10 ⁷ (e ⁻)	---	---	2.5	---
3 x 10 ⁷ (Y)	2.0	---	2.0	3.6
4.6 x 10 ⁷ (e ⁻)	---	---	2.0	---
10 ⁸ (Y)	1.6	3.0	1.5	2.9
3 x 10 ⁸ (Y)	1.1	---	1.0	2.1
10 ⁹ (Y)	0.9	---	0.6	1.3

^aMeasured in supernate of a mixture of 2 g of resin and 10 mL of deionized water.

^bTitrated to pH 7 with NaOH prior to irradiation.

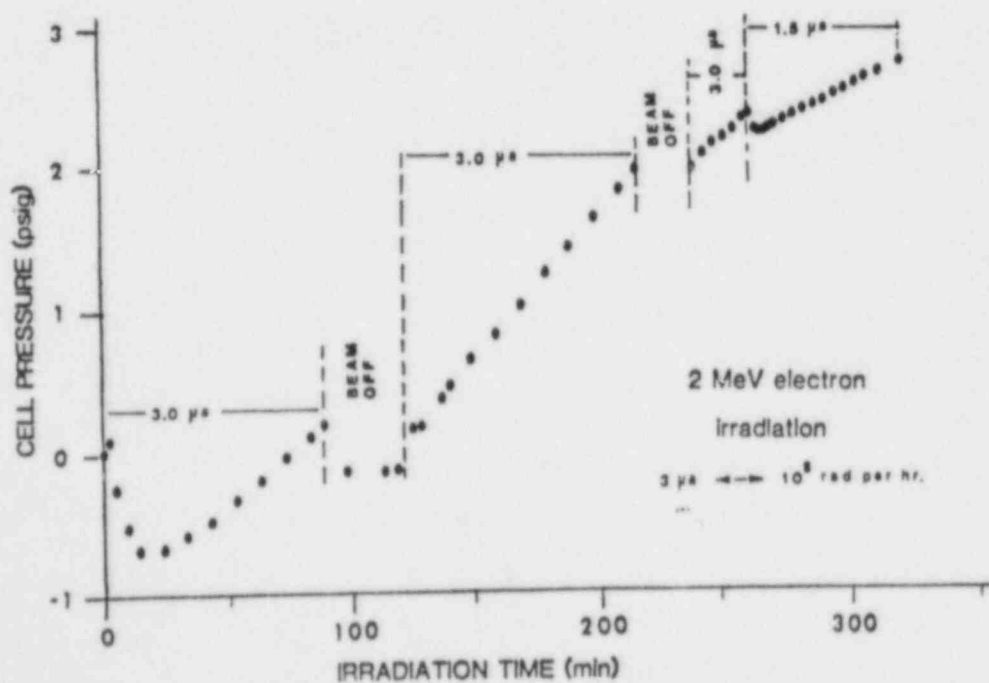


Figure 5.1 Gas generation in IRN-77 resin during electron irradiation. Irradiation temperature = 40°C. Electron beam currents as indicated in μA.

6. SURVEY/CHARACTERIZATION OF FIELD EXPERIENCE WITH HEAVILY-LOADED ION-EXCHANGE MEDIA

The object of this work was to provide a data base for comparison of laboratory and field results on heavily irradiated ion-exchange media. The intent is to learn how well the general trends observed in laboratory experiments are reproduced in field samples. The aim was to determine the validity of laboratory test procedures with respect to predicting field behavior.

Field data are derived from four sources:

- (1) Characterization, at Battelle Columbus Laboratories, of Epicor-II liners PF-16 (Yesso et al., 1982) and PF-3 (Wynhoff and Pasupathi, 1983).
- (2) Data obtained at the TMI site on gas generation in Epicor-II liners.
- (3) Data obtained at ORNL on the resin present in the letdown demineralizer system (LDS) at TMI-II.
- (4) Data obtained at BNL on a core sample from Epicor-II liner PF-3.

6.1 Epicor-II Liners

Epicor-II liner PF-16 contains a mixture of inorganic and organic material, while liner PF-3 is all organic. In each liner, the material is present in three layers. Properties of the material in these liners, including radionuclide and chemical analysis are summarized below.

6.1.1 Epicor II Liner PF-16 Characterization

A report issued by Yesso, Pasupathi and Lowry (1982) entitled "Characterization of Epicor-II Prefilter Liner 16" (GEND-015) describes characteristics of ion-exchange media samples taken from this liner about 18 months after its removal from the decontamination system. We have reviewed this document to provide a data base for examining the correspondence between results observed in ion-exchange media irradiated under laboratory and field conditions.

The reported activity measurements give Cs-137/Cs-134 ratios between 5.6 and 12.5 Ci/Ci in various parts of this bed. The ratio for residual liquid drawn from the liner was 9.8. Assuming an elapsed time of 1.5 yrs between bed loading and the radionuclide assay, we estimate the (average) Cs-137/Cs-134 activity ratio as 5.5 ± 1.8 Ci/Ci. The average initial activity ratio estimated in this way agrees reasonably well with the value (5.234 Ci/Ci) obtained from radiochemical data on the influent water. The relatively large fluctuation in this ratio (+30%) as determined from the radionuclide assay on the ion-exchange media is presumably due to uncertainty in the measurements. Isotopic effects are not expected in bed loading, assuming the feed is well mixed.

Knowing the (average) initial ratio of Cs-134/Cs-137, and the relative Γ -factors (rad/curie) for Cs-134 and Cs-137, the total gamma dose to the ion-exchange media can be calculated from dose rate data obtained for the bed during sampling (Yesso et al., 1982). The beta dose is calculated in a similar manner, assuming that all the beta energy is deposited in the material. The beta dose rate is estimated from the activities reported by Yesso et al. (1982). Contributions from Sr-89 and Sr-90 are neglected. Table 6.1 gives calculated gamma and beta doses, as well as other characterization results for liner PF-16.

Table 6.1
Properties of Ion-Exchange Media in Epicor Liner PF-16^a

Inches From Liner Bottom	Material	Activity ($\mu\text{Ci/g}$)			Calculated ^b Gamma Dose (rad)	Calculated ^b Beta Dose (rad)	Supernatant pH	Present Moisture Content (Air-Dry)
		Cs-137	Cs-134	Sr-90				
32	Inorganic, Zone I	4900	640	1.6	1.5×10^7	3.5×10^7	8.2 ^a	7
30					1.5×10^7			
28					1.5×10^7			
26	Organic, Zone II	730	130	1.4	1.6×10^7	5.3×10^6	3.1	9.3
24					1.6×10^7			
22					1.4×10^7			
20					1.2×10^7			
18	Organic, Zone III	550	44	1.0	1.1×10^7	3.7×10^6	2.2	15
16					1.0×10^7			
14					8.3×10^6			
12	No core sample available				6.7×10^6			
10					4.1×10^6			
8					3.9×10^6			
4					8.6×10^6			
Residual Liquid		.013	.0013	.00052	----	----	5.3 ^d	----

^aData from Yesso et al. (1982) except as noted.

^bCalculated in our program.

^cLiquid measured directly, not as supernate near resin.

^dpH of supernate of 10-mL deionized water over 2-g resin. Final pH of effluent during processing was 2.8.

Estimated beta gamma doses approach 5×10^7 rad in the upper part of the liner (region I). The greater part of this dose is due to beta particles rather than gamma rays. For the lower portions of the liner, (regions II and III) doses are lower and include a relatively larger fraction of gamma radiation. Much of the gamma dose in regions II and III evidently originates from the more highly active region I.

Since ~80% of the observed gamma-emitting radionuclides are concentrated in the first 5 inches of the bed (region I), the beta dose is highly nonuniform within the bed. Most of the gamma radiation produced in region I escapes this layer and is absorbed elsewhere in the bed. If all the gamma radiation generated in region I were absorbed in this layer, the ratio between beta and gamma dose would be .08 for Cs-134 and 0.38 for Cs-137. Since the calculated ratio of region I beta to gamma dose is 2.2, roughly $0.38/2.2 = 17\%$ of the gamma rays are self-absorbed in the thin (5-in.) layer according to the present calculation.

6.1.2 Epicor II Liner PF-3 Characterization

Characterization of a second Epicor-II liner, PF-3, was also carried out at BCL (Wynoff and Pasupathi, 1983). As part of this activity, a core sample of resin was withdrawn from the liner to provide samples for characterization in our program. The sample was withdrawn from the liner as a rectangular core, 1-1/2 in. square by 30 in. long, penetrating the complete depth of the resin bed.

Visual examination of the exposed core surface showed several distinct zones along the core length. Starting from the bottom, the first roughly 6 in. of the core (Figure 6.1) consisted of a layer of amber-grey material which appeared to be moist resin beads. Between about 6 and 18 inches from the bottom (Figure 6.2), the core contained a somewhat lighter amber zone, which is possibly a dryer form of the material found in the bottom 6 inches. Between about 18 and 28 inches from the bottom (Figures 6.3), the core contained a zone inches of darker material, varying in color from brown to reddish brown along its length. The interface between this zone and the adjacent band of amber material (Figure 6.4) is fairly sharp. This fact, and the apparent differences in texture between the material in the amber and dark zones, suggests that the media in the two zones are dissimilar. In particular, the material in the dark zone appears to contain both bead and granular components. The top of the core, between ~28 in. and 30 in. from the bottom (Figure 6.5), consists of a whitish caked material containing embedded resin beads. This material appears to largely cover the upper surface of the bed, as evident from video scans of the bed through the manway access.

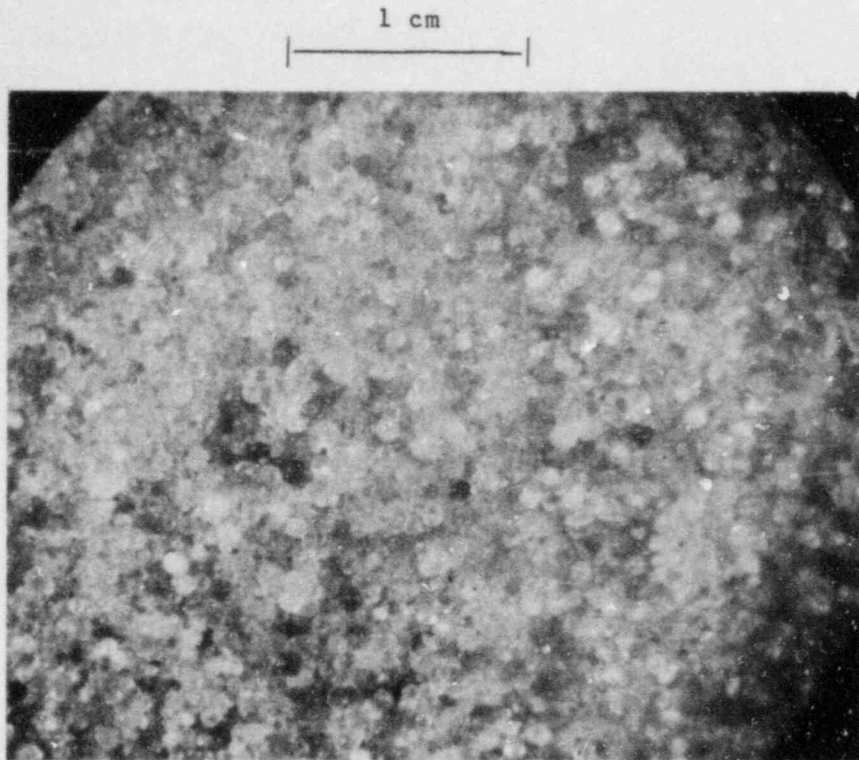


Figure 6.1 Epicor-II PF-3 liner core No. 3, 4 in. from bottom.

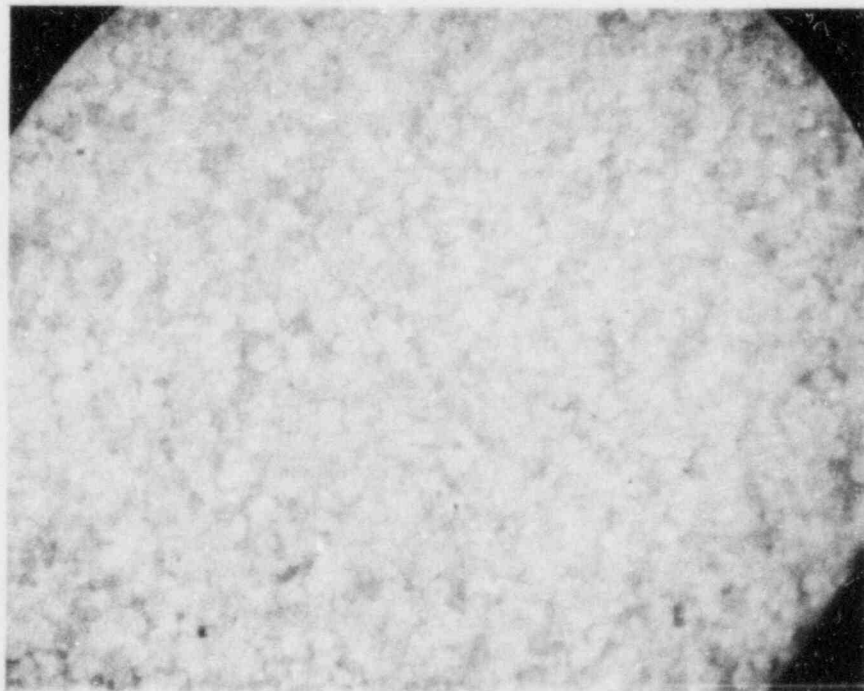


Figure 6.2 Epicor-II PF-3 liner core No. 3, 12 in. from bottom

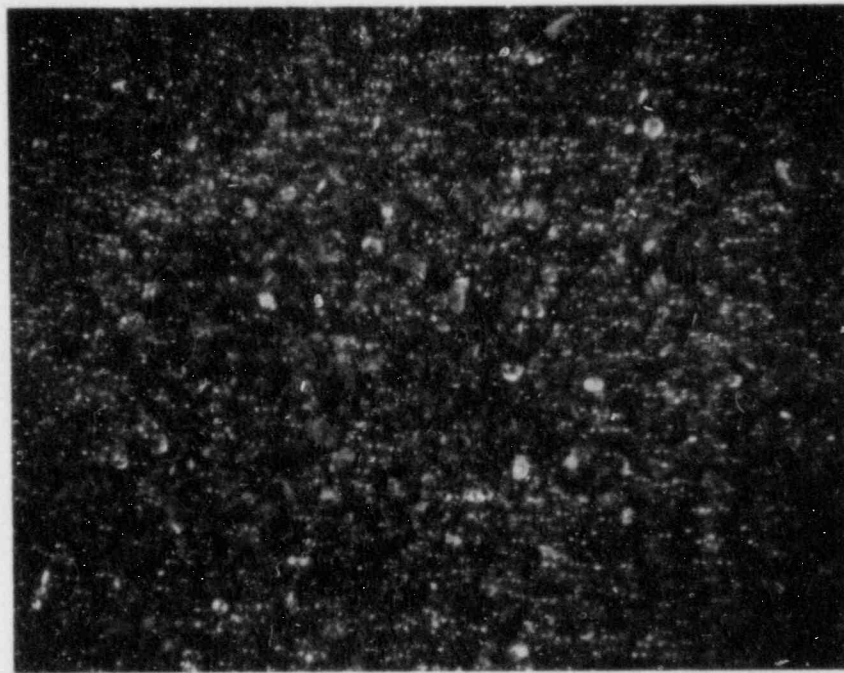


Figure 6.3 Epicor-II liner core No. 3, 24 in. from bottom.

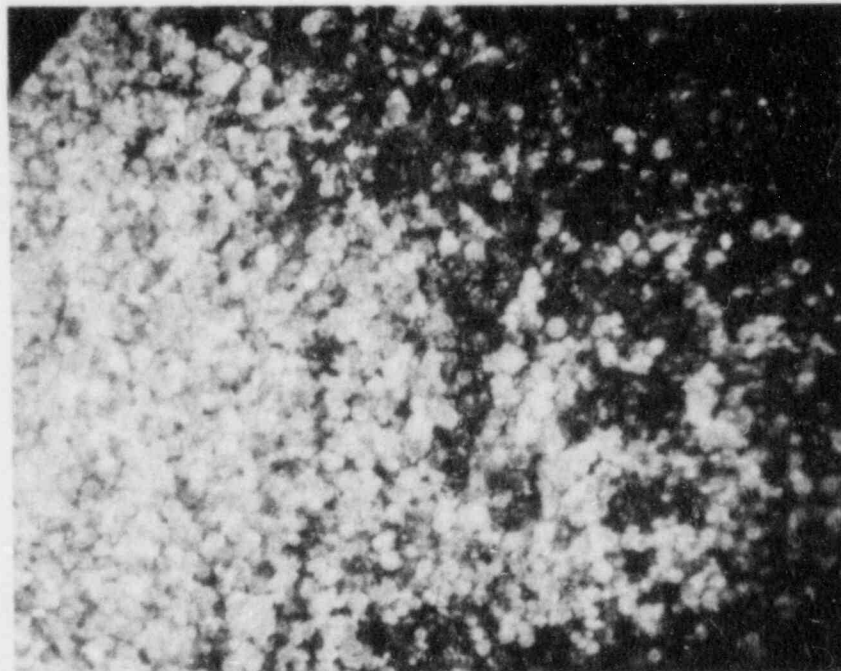


Figure 6.4 Epicor-II liner PF-3 core, 18-1/4 in. from bottom:
interface region between amber and dark brown zones.

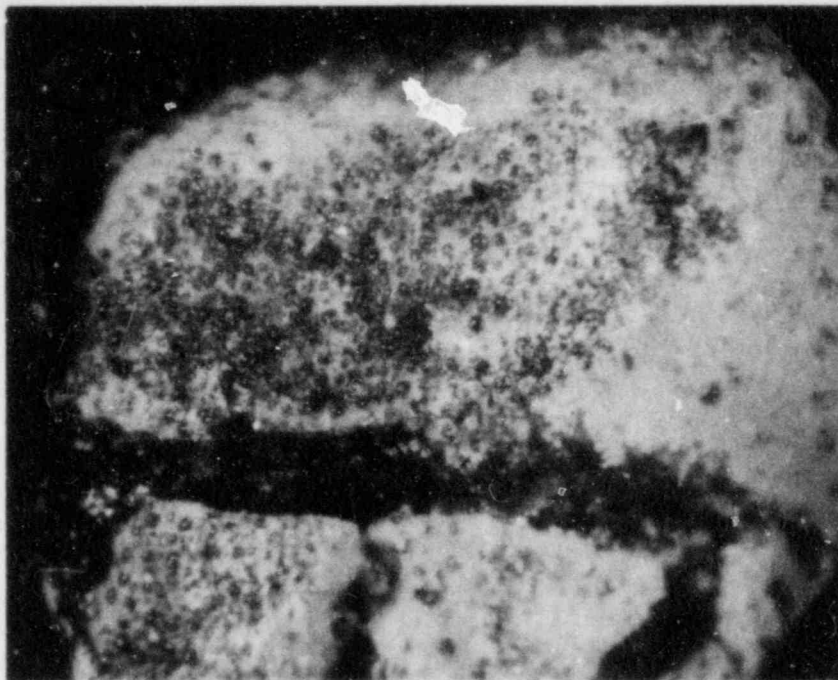


Figure 6.5 Epicor-II liner PF-3 core, 28 in. from bottom.

Cursory examinations of the resin and liner did not indicate any severe degradation due to irradiation. Following the visual inspection, the core was shipped to BNL for further characterization on November 12, 1982. The shipment consisted of 15 separate polyethylene bottles, each containing a separate two-inch section of the core.

Contact radiation level readings on the sample bottles, indicated that the activity was concentrated in a zone extending about 12 in. downward from the top of the core. As noted this zone contains a layer of whitish material at the top, and, below it, a band of darker material about 10 in. thick. Since the radiation dose is localized to some extent in this darker material, part of the coloring might reflect radiation damage. As pointed out, however, at least some of the coloring also reflects intrinsic material properties.

Most of the samples were dry to the extent that they were somewhat difficult to handle - individual beads or particles may be scattered by electrostatic forces. Resin observed during the coring operation appeared reasonably moist - it seems that some dehydration of the samples may have occurred during sampling or storage operations at BCL. In transferring the resins from the polyethylene bottles to small sample jars there was no evidence of any gross physical deterioration (agglomeration, etc.) of the resin.

Several small (~1 g) samples were taken from each separate 2-in. section of the core. One series of samples was contacted with deionized water in the ratio 1 g to 10 mL. The pH of the aqueous supernate was measured ten hours after the resin was contacted with the water, and again after a contact time of 30 days. A syringe was then used to withdraw 1 mL samples of the supernate through a 4.5-micron filter. The filter was necessary to remove suspended fragments of the ion-exchange media from the supernate. The 1 mL samples withdrawn in this manner showed no observable coloring. One group of supernate samples was then used for determination of activity in solution. A second group of samples was set aside for characterization of soluble decomposition products such as sulfates.

Several beads (~2-30 mg) were removed from each core section and taped to sample discs. Gamma scans and microscopic examination were carried out on these samples. Counting efficiencies were determined with a standard source of similar geometry*. In view of the small sample size, the absolute values should be considered rough estimates. The data, however, clearly indicate that most of the cesium activity is concentrated at the top of the bed. The estimated maximum Cs-137 activity determined from the small samples, ~900 $\mu\text{Ci/g}$, is lower than that reported by BCL for bulk samples taken from a different core of the same liner (Table 6.4). The average ratio of Cs-137 to Cs-134 activity in the BNL small resin samples was $14.2 \pm 10\%$ for samples 1-15. This seems to be in agreement with operating records for the Epicor II system.

Beta radiation dose estimates similar to those in Table 6.1, were also made for liner PF-3. Radiation dose estimates and the results of various characterization of the media in liner PF-3 are collected in Table 6.2.

Estimated beta-gamma doses are approximately 7×10^7 rad in material near the top of the liner. In this region as mentioned earlier (Swyler and Dayal, 1983) the low pH levels are at least suggestive of some radiation damage.

Gas generation data from Epicor-II liners has also been studied. In all cases, oxygen is rapidly depleted from the atmosphere over irradiated ion-exchange media. We estimate, from data obtained by Yesso (Yesso et al., 1982) and our own dose calculations, that a dose of 1.2×10^8 kg-rad was sufficient to remove 7 liters of oxygen from the atmosphere over Liner PF-16. The principal radiolytic gas is hydrogen. Estimated hydrogen generation rates in liner PF-3 are $9.9 \text{ cm}^3/\text{h}$ based on data reported by Sheff (1982).

*NBS mixed radionuclide gamma ray emission point source standard 4125-6 No. 106. The assistance of J. Steimers (BNL's Safety and Environmental Protection Division) in counting the samples is gratefully acknowledged.

Table 6.2
Properties of Ion-Exchange Media in Epicor-II Liner PF-3

Inches From Liner Bottom	Material	Activity ^a ($\mu\text{Ci/g}$)			Calculated ^a Beta Dose (rad)	Supernatant pH		Supernatant Activity ^b ($\mu\text{Ci/g}$) Resin		Supernatant Sulfate Moles/g of Resin	Present Moisture Content ^a (Air-Dry)	Relative Resin Activity $\frac{\mu\text{Ci/g}}{\text{Cs-137}}$
		Cs-137	Cs-134	Sr-90		(1)	(2)	Cs-137	Cs-134			
30 - 28					----	----	----	----				----
28 - 26						2.7	2.6	29	1.9			400
26 - 24	Organic						2.8	31	1.8	1×10^{-4}	18	900
24 - 22	Zone I	5000	280	200	7×10^7	3.0	3.1	20	1.4			800
22 - 20							2.9	5.6	0.4			520
20 - 18							3.2	2.4	0.13			14
18 - 16							2.6	0.5	0.04			10
16 - 14	Organic						2.7	0.2	0.01			2.1
14 - 12	Zone II	5.0	0.3	0.3	7×10^4	3.0	2.7	0.1	0.007	3×10^{-5}	30	2.7
12 - 10							2.8	0.02	0.001			0.8
10 - 8							2.6	0.002	----			0.2
8 - 6							4.9	----	----			0.2
6 - 4	Organic	2.0	0.3	0.3	5×10^4	5.1	4.7	----	----	7×10^{-7}	45	0.1
4 - 2	Zone III						4.7	----	----			1.7
2 - 0							4.8	----	----			1.5
Residual Liquid		0.42	.0021	.001		5.3				1.6×10^8 moles/l.		

^aSample 1 - Core analyzed at Battelle Columbus Laboratory.

^bSample 2 - Core analyzed at Brookhaven National Laboratory.

6.2 LDS Resins From TMI-II

Data obtained from this analysis of the resins in the letdown demineralizer system at TMI are still being compiled by personnel at ORNL and GPU (Quinn, 1983). It is estimated that these resins were exposed to a dose on the order of 10^9 rad and reached a temperature of $\sim 400^\circ\text{C}$. The resins are generally similar to the material used in the present experiments. An analysis of radiolytic decomposition products is given in Table 6.3 (Malinauskas, 1983).

Table 6.3
Decomposition Products in Liquids and Solids (Resins) from
the B2 Letdown Demineralizer System at TMI-II (Malinauskas, 1983)

Decomposition Products (ppm)	B-2 Liquid	B-2 Solid
B	3000	>200
C	900	>10%
Na	$\sim 10,000$	>1000
Mg	<1	2
Al	10	70
Si	<3	<5
P	0.1	<1
SO ₄	6000	15,000
Cl	20	30
K	0.8	4
Ca	10	30
V		1
Cr	0.6	5
Mn	0.1	5
La		3
Ba		<1
Cs	30	100
I-129		
Te	<1	30
Sn		~ 2
In	0.3	30
Cs	<1	60
Ag	2	30
Rh		<3
Mo		
Nb	<.1	<1
Zr	1	6
Sr	<1	1
Rb	4	15
As	<.5	<1
Zn	0.2	<1
Cu	0.3	<1
Ni	0.6	40
Co	<.1	<1
Fe	10	200
U	0.109	283
pH	5.3	

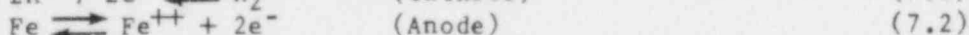
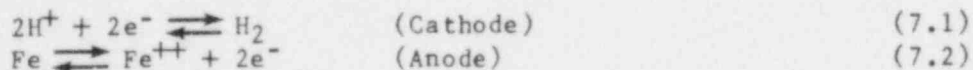
7. DISCUSSION AND SUMMARY

Experimental results described in Sections 3 through 6 are discussed in this section. The discussion has two objectives: to interpret the results, as far as possible, in terms of basic mechanisms; and to apply these results, and their interpretation, to the evaluation radiation effects in radwaste resins for regulatory purposes. At the end of this section, results from this report, and from work described in an earlier topical report, are combined to define recommended test procedures and identify logical regulatory criteria.

7.1 Enhanced Mild Steel Corrosion in Irradiated Ion-Exchange Media

Corrosion in irradiated ion-exchange media is a complex process, involving inhomogeneous conditions at the metal resin interface, (which may tend to promote pitting of crevice corrosion), competing reactions for radiolytic species and corrosion products, transport processes within the medium, etc. It is not possible to give a detailed electrochemical interpretation of the corrosion process. The discussion here will be largely phenomenological.

Corrosion rates are found to vary considerably with resin loading and with moisture content. For hydrogen form resin, the correlation between corrosion weight loss and hydrogen gas evolution indicates typical acid attack. The anode and cathode reactions would be

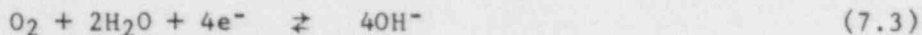


Based on earlier work (Swyler, Dodge and Dayal, 1983), we believe that the acid involved in the corrosion in irradiated H^+ form resin is sulfuric acid. Kendig and Isaacs (1982) identified sulfuric acid resulting from thermal decomposition of H^+ form sulfonic acid cation resin as being responsible for corrosion in Alloy 608. Corrosion rates in H^+ form resin are ~ 0.07 $\text{mg}/\text{cm}^2\text{-h}$ after ~ 200 h. This rate is in reasonable agreement with extrapolated values for mild steel in 0.1 normal H_2SO_4 (Mathur and Vasudevan, 1982).

For other resin forms, interpretation of the corrosion rate is less straightforward. Corrosion rates are lower for Na^+ , HOH and NaCl form resins than in H^+ form resin. To the extent that corrosion in irradiated resins is analogous to corrosion in aerated aqueous solutions, corrosion rates should decrease as the resin pH increases (c.f. Uhlig, 1948). For irradiated samples without corrosion coupons, resin supernatant/free liquid pH increases in the order $\text{H}^+ < \text{NaCl} < \text{HOH} < \text{Na}^+$. However, corrosion in Na^+ form resin is greater than that in NaCl or HOH forms. In the HOH and NaCl forms, the corrosion coupon is also in contact for some time with free liquid. At the pH observed in Na^+ , NaCl and HOH resin supernates, one would also expect hydrogen gas generation in the aqueous corrosion of mild steel in aerated solutions (Uhlig, 1948; Hovey, 1980). However, additional hydrogen gas generation did not clearly accompany corrosion in all cases for NaCl, HOH or Na^+ resins. In short, while acidic species are certainly involved in the corrosion

process as indicated by the elevation of supernatant pH in samples containing corrosion coupons, we cannot conclude that the corrosion process is entirely governed by the radiolytic pH changes.

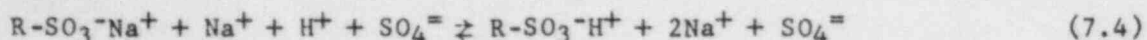
Other factors beside radiolytic pH changes which affect corrosion rates are oxygen and moisture content. In aqueous systems containing dissolved oxygen, corrosion rates may be accelerated by the cathodic (depolarization) reaction



Other oxidizing species (peroxides, perchlorates, nitrates etc.) may also participate in the cathode reaction. Atmospheric oxygen is rapidly depleted when resins are irradiated in a closed environment. Consequently, if corrosion rates are controlled by a reaction such as 7.3, corrosion should increase when samples are irradiated in an open system. This is the case for Na⁺ form resin; radiolytic corrosion rates in H⁺ form resin are less sensitive to atmospheric conditions. We conclude that, for H⁺ form resin, the cathodic reaction is probably (7.1), while for Na⁺ form reaction (7.3) may contribute also.

Lack of gaseous hydrogen evolution during corrosion in Na⁺, HOH and NaCl form resin would be consistent with a cathode reaction such as (7.3). Corrosion would then be decreased if radiolytic oxidation of the resin tends to produce a reducing environment. It is likely that the difference in corrosion rates between these experiments and those in earlier measurements (Gangwer and Pillay, 1982; Barletta, Swyler and Davis, 1982) partly reflect differences in oxic conditions--earlier irradiations were carried out in open systems. However, corrosion continues long after the time (< 100 h) oxygen was no longer detectable in the atmosphere over irradiated resins. Other reactions must account for this fact, and for the pH increase accompanying mild steel corrosion.

A plausible model to account for the corrosion behavior of fully swollen Na⁺, NaCl and HOH resins should consider the competition between the radiolytic generation of corrosive species uptake of these species in corrosion, and the ion-exchange properties of the resin. For Na⁺ resin at high radiation dose rates, local conditions may become sufficiently acidic to permit cathodic hydrogen gas generation [reaction (7.1)]. The local acidity is determined by the balance between acidity generated within the resin and the release of H₂ at the cathode. Since column pH measurements do not indicate extensive pH gradients in the resin, H⁺ depletion due to corrosion may be fairly uniform within the bed. At the same time, iron ions produced by corrosion remain relatively localized near the surface of the corrosion coupon (< 2 cm away in these experiments). Also, sulfate ion concentrations remain reasonably uniform throughout the bed. A more extensive depletion of H⁺ can be rationalized with the local accumulation of Fe⁺² or Fe⁺³ if it is assumed that a significant fraction of the radiolytic H⁺ is bound to undamaged sites of the resin. This is in agreement with previous results (Swyler, Dodge and Dayal, 1982). Thus the pH can be adjusted locally, in response to H⁺ uptake at the corrosion coupon, by a shift in the equilibrium:



If this process in fact operates, it has several important implications:

- The H^+ uptake determined by comparing supernate pH measurements with and without corrosion coupons, will underestimate the H^+ actually consumed in corrosion, since pH measurements do not directly indicate the amount of H^+ on undamaged sites in the resin.
- The ion-exchange mechanism, 7.4, provides a means of locally changing the pH without requiring the long-range diffusion of Fe ions to maintain charge neutrality. The transport of Fe ions thus will not be a rate limiting factor in corrosion.
- The corrosion rate at the coupon may set the pH for resin at least several cm from the coupon. As the pH is decreased by irradiation, the corrosion rate will increase until a steady state is achieved at which radiolytic H^+ formation rates equal H^+ uptake rates in corrosion. The time and pH values at which this occurs will depend on resin volume and radiation dose rate (radiolytic H^+ generation) and on the corrosion coupon size and the relation between pH and corrosion rates (H^+ uptake).

The hypothesis presented above accounts for several qualitative features of the experimental results. In particular, the pH vs. contact time curves for irradiated resins with corrosion coupons show a minimum which is clearly suggestive of two competing processes. For the mixed bed resins, corrosion rates are fairly low until this minimum is achieved (which occurs at about 500 h for a dose rate of 1.6×10^6 rad/h). Subsequently, the corrosion rates are greater than those for Na^+ form resin. In the mixed bed systems, which release free liquid upon irradiation, and in resin-water slurries, radiation corrosion is somewhat more uniform than in fully swollen resins. For the mixed bed and resin water systems, it is possible that the minimum pH reflects conditions at which a surface film becomes soluble in the aqueous environment. During irradiation, similar constraints apparently do not apply to fully swollen cation resins.

To maintain a critical perspective, it must be pointed out that we are not yet able to identify the rate limiting process in radiolytic corrosion. This is partly due to the fact that, due to programmatic limitation, the chemical nature of the corrosion products was not determined in detail. The presence of iron sulfates would indicate typical "strong" acid corrosion; and sulfate transport could ultimately limit corrosion rates. There is no clear evidence, however, that radiolytic sulfate levels in the resin are affected by corrosion. Alternatively, corrosion products such as iron hydroxides or oxides would indicate a cathodic reaction involving an oxidizing species such as reaction (7.3). In this case however, a source must be postulated for the oxidizing agent. While this is not straightforward, it is possible that the

oxidant could be some radiolytic species. For example, we believe that radiolytic H_2 production in fully swollen cation resins involves water radiolysis (Swyler, Dodge and Dayal, 1983). Oxidizing species (e.g. H_2O_2) produced in this reaction could also contribute to cathodic depolarization.

From a practical standpoint, penetration data for mild steel corrosion in irradiated resins are summarized in Table 7.1.

Table 7.1
Estimated Average Penetration of Mild Steel by Corrosion in Resins Irradiated to a Dose of 10^9 rad.

Resin Form	Irradiation Condition	Irradiation Dose Rate (rad/h)	Contact Time (h)	Average Penetration (cm)
H^+	Fully Swollen (s)	1.6×10^6	600	1.4×10^{-2}
H^+	Dry (s)	1.6×10^6	600	0
H^+	Slurry	1.6×10^6	600	7.1×10^{-3}
Na^+	Fully Swollen (s)	1.6×10^6	600	3.5×10^{-3}
Na^+	Fully Swollen (s)	1×10^5	10,000	1.1×10^{-2}
Na^+	Fully Swollen (s)	4×10^4	25,000	1.8×10^{-2}
Na^+	Dry (s)	1.6×10^5	600	0
Na^+	Slurry	1.6×10^5	600	2.8×10^{-3}
HOH	Fully Swollen (s)	1.6×10^6	600	1.2×10^{-3}
NaCl	Fully Swollen (s)	1.6×10^6	600	1.5×10^{-3}

These data of course refer to the particular experimental conditions in this program. Also, corrosion is not entirely uniform. Particularly in unirradiated H^+ form resin, pronounced pitting was observed. Interestingly, in irradiated resins the attack tends to become more uniform. This is in agreement with the earlier observations of Barletta, et al. (1983) and may involve solubility effects on corrosion films. In irradiated H^+ resins, the coupon was attacked preferentially at grain boundaries produced in the rolling process. Taking these factors into account, and assuming a typical observed pit density of ~ 200 pits/cm² and a pit of ~ 300 μ diameter bounds the maximum penetration at $\sim 9 \times 10^{-2}$ cm for H^+ form resin at 600 h. This is obviously conservative, since it exceeds the coupon thickness, and the coupons were not penetrated.

7.2 Comparison of Field Data and Laboratory Results

7.2.1 General Observations

Direct comparison between results for the Epicor-II system and laboratory data is not possible, due to the proprietary nature of the Epicor ion-exchange media. Liner PF-16 is known to contain both inorganic (zeolite) and organic ion exchangers. We may assume that this upper zone is inorganic (zeolite); the lower zones are presumably organic (Yesso et al., 1982) sulfur present in zones II and III may indicate the presence of a sulfonic acid functional group on cation resin.

For liner PF-3, sulfur was found in material from all three zones (Wynhoff and Pasupathi, 1983). Sodium was clearly evident in the material in zone I and trace sodium signals were observed in material from zone II. Only material from zone I showed evidence for significant amounts of other metal ions (Fe, Si, Al).

From these observations and the media pH data reported earlier, we suggest the following correspondence for the ion-exchange media in liners PF-16 and PF-3.

PF-16		PF-3	
Region	Media	Region	Media
Zone I	Zeolite	No analog	No analog
Zone II	Cation	Zone I	Cation
Zone III	Mixed Bed	Zone II	Mixed Bed
Bottom	Anion	Zone III	Anion

7.2.2 Epicor-II Liner PF-16

Based on the correspondence suggested above, several general comparisons can be made. The data for liner PF-16 could be compared to those obtained by Barletta et al. (1983) in their scoping studies. These experiments, however, were carried out on material in which the different ion exchangers were thoroughly mixed. Further, the samples were irradiated in an air environment, at greater dose rates ($\sim 1 \times 10^6$ rad/h) and greater total dose ($>10^8$ rad). The isotropic irradiations of Barletta et al. would not be expected to reproduce the relative amounts of irradiation damage to these media in liner PF-16. There is also no simple way to relate the pH data in these experiments to the values for the individual media in Table 6.1.

Barletta et al. observed enhanced corrosion of mild steel coupons contacted with "D-mix" during irradiation. Again, comparison is complicated by the homogeneity of the D-mix samples. For liner PF-16, material in zone III showed a pH of 2.2. The mixed material (D-mix) showed a pH of ~5.4 at 10^6 rad. Residual liquid at the liner bottom had a pH of 5.3. This may be more representative of what is expected when the different components interact, and more closely resembles the laboratory values in mixed material.*

Barletta et al. observed the formation of calcium sulfate (gypsum). Presumably, the sulfate was released in the decomposition of sulfonic acid cation resin in the "D-mix." At the estimated doses for the organic media in PF-16, based on our experiments on sulfonic acid resin, a release of about 10^{-5} moles-per-gram would be expected. Little sulfate was found in the residual liquid of liner PF-16. Possibly sulfate found in zone III might have originated in decomposition of material in zone II.

Gas generation data on laboratory samples are in qualitative agreement with field observations in liner PF-16. Radiolytic oxygen scavenging is observed and hydrogen gas is generated. Only a crude comparison can be made between the absolute rates. In the liner PF-16, we estimate an average G-value of ~0.4 for hydrogen generation. Barletta et al. found a G-value of ~0.25 in their laboratory measurements.

Other observations (liner corrosion, microscopic examination of media, etc.), were also carried out at BCL. No significant physical degradation of the media was reported. Corrosion was observed on areas where the liner surface was not covered with a corrosion-resistant coating. These visual observations are in general agreement with the laboratory experiments in that irradiation to 10^8 rad did not produce a gross degradation in the physical properties of D-mix.

7.2.3 Epicor-II Liner PF-3

For liner PF-3, a somewhat more detailed comparison of field and laboratory data is possible. Again, however, the exact nature of the material in the liner is proprietary.

The pH values and supernatant sulfate levels in zone I (Table 6.2) are actually in rather good agreement with those expected for sodium form sulfonic acid resin at 7×10^7 rad. In zone II, the supernatant sulfate yield ($\sim 3 \times 10^{-5}$) is reasonably consistent with a dose of $\sim 2 \times 10^7$ rad to sulfonic acid resin based on laboratory results. Residual liquid taken from the liner again has a pH which is much greater than that found for deionized water in contact with media from zone I or II. This either indicates a buffering effect in zone III, or that radiolytically-produced acidic species in zones I and II are not transported to the free liquid in the bottom of the liner.*

*In fact, if the bottom of the liner contained either an anion resin in OH^- form, or a buffering agent such as aluminium hydroxide, the difference between the pH of the residual liquid and the media in zone III may be accounted for.

In zone I, some of the beads are cracked in half. In zones II and III, some of the beads had cracked in half, while others exhibited surface fracture. Cracking effects similar to those in the media of PF-3 have been produced by irradiation in our experiments (due presumably to differences in cross-linking behavior and resin moisture content). Media in the bottom of zone III visually appeared moist when the core was withdrawn. If this is an anion resin some of the moisture could have been due to free liquid release as found in our experiments. These comparisons are speculative, however; probably the most significant observation regarding structural damage is that agglomeration of the media was not observed. This is in agreement with laboratory experiments under similar conditions.

In PF-3, corrosion of the liner was observed where the material at the top of zone I was in contact with the liner wall at points where the protective coatings had blistered or spalled off the wall. The extent of the corrosion in PF-3 was not easily quantified (although apparently not extensive). So comparison between field and laboratory data is difficult. In Na^+ form sulfonic acid resin, in contact with mild steel for three years at a dose rate of 4×10^4 rad/h (rather than 3×10^3 rad/h), we would expect a net weight loss of ~ 100 mg/cm². This is not extensive.

Assuming that all the hydrogen generation occurs in the heavily loaded material in zone I, published gas generation data lead to a rough estimate G-value of about 0.7. Measured values for polystyrene-DVB resins range between 0.13 and 0.35 in our work for cation and anion resin, respectively. Including gas generation resulting from other parts of the liner would reduce the field G-value to about 0.5 which is still greater than lab values.

For liner PF-16, a lower bounding estimate can be made for oxygen scavenging. We estimate that this bound corresponds to an oxygen uptake of $\geq 6 \times 10^{-8}$ L/kg-rad. Our experimental numbers for sulfonic acid resin at high dose rates are $\sim 3 \times 10^{-7}$ L/kg-rad. Since the O_2 scavenging is non-linear with dose (Swyler, Dodge and Dayal, 1982; Capolupo and Sheff, 1982), most of the dose to the liner is administered to inorganic material (zeolite) and the dose estimates in the liner are very rough, we believe the quantitative agreement between lab and field data oxygen scavenging is reasonable.

7.2.4 LDS Resins From TMI-II

For these resins, both radiolytic and thermal degradation probably occurred. The temperature range to which these resins were subjected has not been investigated in the present program. Russian workers (Tulupov et al. 1981) have studied the combined effects of radiation and heat on sulfonic acid cation resin decomposition. Interestingly, they find that the two processes are not equivalent, and that thermal decomposition tends to produce less acidic condition.

Data in Table 6.3 may support these arguments. High sulfate concentrations in LDS resins probably indicate the decomposition of sulfonic acid cation resin. The LDS liquid pH (5.3) is significantly greater than the pH (~1) which would be expected from sulfuric acid or bisulfate salts at the indicated sulfate levels produced by the radiolysis of sulfonate groups. Consequently, either the sulfate in the LDS resins is produced by a process which is not analogous to our laboratory experiments (e.g. thermal decomposition) or the radiolytic acidity is somehow buffered or neutralized (perhaps by borate) in the field samples.

7.2.5 Summary

Very little can be learned about the detailed behavior in a multi-component, stratified field sample, such as liner PF-16, from laboratory experiments in which the components are mixed homogeneously and irradiated isotropically. In general, one must understand the radiation damage susceptibility of each component, and the interactions between the components in the field configuration which is applicable. A detailed comparison of Epicor-II data and laboratory data is difficult because of the proprietary nature of Epicor-II media and because of a lack of knowledge of the properties of the unirradiated material. Some general comparisons can be drawn as follows:

- At the estimated radiation doses for liner PF-3, the general physical state of the field ion-exchange media is not severely degraded. This is in agreement with laboratory studies.
- Laboratory studies indicate that a limited amount of corrosion should occur in PF-3. This is observed.
- The pH and sulfate levels in the supernate of liquids contacting media from zone I of PF-3 are in reasonable agreement with laboratory results for irradiated sodium form sulfonic acid resin.
- The correlation between supernate pH and sulfate levels for the media in zone II is difficult to rationalize in terms of degradation of Na⁺ form sulfonic acid resin.
- Specific radiolytic hydrogen yields (G-values) and oxygen scavenging rates estimated from field data are not grossly disparate with those measured for polystyrene-divinylbenzene resins in the laboratory.

It must be pointed out that, with the exception of radiolytic gas generation and uptake, there is no unambiguous evidence that any of the effects mentioned for the field samples (sulfate in solution, cracking of the beads, pH levels, etc.) are actually caused by irradiation. For example, in the liner PF-3, the Cs-137 content of the resin is ~5000 mCi/g. The Cs level in the supernate corresponds to a release of less than 0.1% of this material. At a dose of $\sim 7 \times 10^7$ rad, one expects a damage of <2% of the exchange sites in sulfonic acid resin. Unless the Cs⁺ protects the resin site (for which

we have no evidence) or is taken up again at an undamaged Na⁺ site (for which there is some evidence; S. Reilly, private communication), the supernate activity data are not easy to reconcile with radiolytic attack (or any other form of attack) on the functional group.

7.3 Conclusions and Recommendations

In this section major conclusions from the present report are summarized. These are combined with certain results described previously (Swyler, Dodge and Dayal, 1983) to arrive at recommendations for assessing the effects of irradiation on radwaste containing organic ion-exchange media.

1. Fundamental radiolytic decomposition processes in irradiated ion-exchange resins include scission of the functional groups, radiolytic gas generation, release of free liquids, and radiolytic oxidation. Factors affecting the fundamental decomposition process include resin loading, resin moisture content, irradiation dose and atmospheric oxygen content. Except where radiolytic oxidation is involved, the fundamental radiolytic processes are not particularly sensitive to irradiation dose rate, or to the difference between gamma and beta irradiation. Consequently, for conditions appropriate to resin storage in a closed environment, simulation of internal radiation doses by high dose rate external gamma radiation, according to present NRC guidelines (MacKenzie et al., 1982), is apparently a valid procedure for assessing fundamental radiolytic decomposition (see also Conclusion 7).
2. Both resin degradation and radiolytic corrosion may be significantly reduced under anoxic conditions (i.e., in a sealed system where oxygen is quickly scavenged by radiolytic processes). Test conditions appropriate to a particular application should reproduce the expected atmospheric oxygen environment as well as possible. This has not always been done in resin testing for radwaste disposal considerations.

The magnitude of radiolytic oxidation effects on resin decomposition and radiolytic corrosion is not easy to generalize. Upon further consideration it may be useful to apply a regulatory limit to the amount of oxygen to which the resin can be exposed during storage. The kinetic data obtained earlier (Swyler, Dodge and Dayal, 1983; Sheff, et al., 1982; Barletta et al., 1982) may lend themselves to establishing such a limit. A major question which could require further study is the thermal and chemical stability of radiolytically oxidized resins, particularly in view of recent field experience (Piciulo et al., 1984).

3. A fundamental process which may be of particular interest in regulatory application is radiolytic scission of the resin functional group. In sulfonic acid cation resin the mechanism of this process lends itself to regulatory criteria in a straightforward manner--sulfate ion is produced with a fairly well-defined yield, or G-value,

which can be bounded for a wide range of external conditions. This supports the reasoning applied by MacKenzie et al., in reviewing published yield data to arrive at regulatory criteria for resin irradiation doses.

The present data indicate that sulfate yields can be measured fairly simply in the supernate of deionized water-irradiated resin solutions. Results obtained in this way did not differ greatly from those for irradiated resin-water mixtures. Also, at least for resins irradiated in closed systems, yields measured in supernates over irradiated resin do not indicate a pronounced concentration dependence, or long-term (>2-3 weeks) aging effects. Consequently, while properties of resin-water solutions are most directly relevant to radwastes consideration, yields obtained by rinsing the resin (∞ dilutions, zero aging) are probably also meaningful. This should be verified for a particular application, however. Finally, it should be recognized that neither supernatant nor rinse measurements reproduce the actual conditions in an individual resin bead during irradiation.

4. As a consequence of radiolytic attack on the functional group in cation resin, counterions are released and acidic species produced. Formation of acidic species in cation resin, for other than H^+ loading probably involved H^+ produced in the radiolytic oxidation of $-SO_3^-$ to $SO_4^{=}$. Other mechanisms could also contribute, including scission of the resin back bone. The important point is that, whatever the process, the radiolytic acidity depends on a number of factors beside the $SO_4^{=}$ yield and is not easy to predict in detail. For monovalent cation loading the irradiated resin is less acidic than the corresponding bisulfate, due to ion-exchange processes at undamaged resin sites.
5. Irradiation induced acidity will generally promote corrosion of mild steel contacted with resins during irradiation. (Similar effects have been observed in stainless steel by McFarland [McFarland, 1982]). The corrosion process is complex, and the role of H^+ in the corrosion process, for other than H^+ from resin has not been unambiguously identified. Prediction of total corrosion from mass balance consideration (Hovey, 1980) may be misleading unless the presence of radiolytic H^+ on the undamaged exchange sites resin is accounted for, or the contribution of radiolytic oxidants understood. Corrosion rates and net corrosion in the present experiments is rather modest. It is important to point out, however that, for a given radiation dose, net corrosion increases as the radiation dose rate decreases--dose rate effects must be considered in corrosion experiments. Also, because of transport properties, it is not meaningful to simulate radiolytic corrosion with resins-sulfuric solutions.

6. Interestingly, at high dose rate and moderate doses ($<5 \times 10^8$ rad) there is no clear evidence that corrosion is promoted when free liquids are released from irradiated mixed bed resins, or when coupons are irradiated in cation resin-liquid slurries. This is potentially significant since, at the present allowable radiation dose limit (10^8 rad) irradiated mixed bed resins may release free liquid. As indicated earlier, however, it is difficult to generalize on corrosion effects, and particularly on the effective bed volume which may contribute to corrosion. Iron corrosion products apparently interact with only the first few centimeters of material near the corroding surface (at least in short-term experiments) but corrosion could affect resin pH over greater distances. Consequently, any test for corrosion resistance of container material in irradiated resin must specifically consider the ratio of metal surface to resin volume. The available information, is not sufficiently complete to suggest a standard test procedure. An evaluation of results for two different ratios, say 5 cm^{-1} and 50 cm^{-1} , is recommended to scope surface area to volume ratio effects..

7. The conclusions and recommendations listed above are based largely on the results of laboratory studies. In this program some effort was directed toward determining how well laboratory data obtained on samples exposed to external irradiation reflected the results of field samples subjected to internal irradiation. Unfortunately, it is not possible to make a definitive statement on this point, due to the proprietary nature of the field samples, and uncertainty regarding initial conditions. Some general observations can be made, however. First, analysis indicates that in stratified field samples, the majority of the local radiation dose can be due to beta particles. Laboratory experiments suggest that the bulk effects of internal beta irradiation can be adequately simulated by external gamma radiolytic irradiation. Second, gas generation behavior in field samples agrees at least qualitatively with that observed in the laboratory. Third, observations on the (lack of) physical degradation in field samples correspond to observations on laboratory samples irradiated under anoxic conditions. Fourth, the correspondence between radiolytically produced chemical changes (pH, etc.) in laboratory samples and in field samples is difficult to establish. If anything, conditions in field samples tended to be somewhat less acidic than in laboratory experiments. Taken together, these observations provide no systematic evidence that laboratory testing using external irradiation is not a valid procedure.

8. For future field or laboratory evaluation involving proprietary material it is recommended that samples of unirradiated material be provided for comparison, in a configuration reflecting field conditions. All radiation damage experiments could then be made only to study changes in the material, which should not be proprietary.

9. There are several experiments which could shed additional light on the extent of radiation damage in Epicor-II resins. A number of these were, in fact, planned in the present task, but were not completed due to programmatic restrictions. These still appear to be worth doing and include:
- An absolute radionuclide inventory to the different segments of BNL's core from liner PF-3. Only relatively small sample data are now available.
 - A more detailed radionuclide and chemical analysis of the supernate over irradiated resins. This would include organics, cations such as sodium, and anion such as borate.
 - A determination of the chemical loading on the media. This can be done by determining the principal cations or anions present following acid digestion of the media for radionuclide analysis.
 - Determination of the amount of sulfate which is bound in the resin (by rinsing and ion-exchange process, followed by colorimetric analyses of the supernate).
 - Determination of the irradiation damage response of the media in the various zones to external gamma irradiation. This would include measurements (gas generation, soluble decomposition products, irradiation corrosion, etc.) similar to those carried out on polystyrene-DVB resins under Task 3. These experiments would provide at least some data to determine what effects, if any, a dose of $\sim 7 \times 10^7$ rad might have produced in the field by applying the same incremental dose in the laboratory and measuring changes.
 - Measurement of the gas generation [long-term due to self-irradiation in small samples (~ 50 g) from zone I].

8. REFERENCES

- Armitage, G. M. and S. J. Lyle, "Mass Spectrometric Study of the Deterioration of Polystyrene-Based Ion Exchangers," Talanta, 20, 315, 1973.
- Barletta, R. E., K. J. Swyler, S. F. Chan, and R. E. Davis, Brookhaven National Laboratory, "Solidificaiton of Epicor-II Waste Products," BNL-NUREG-22931R, 1982.
- Capolupo, W. and J. R. Sheff, "Radiolytic Gas Generation and Oxygen Depletion in Ion-Exchange Materials," Materials Research Society Symposium Proceedings 15, 447, 1983.
- Clough, R. L. And K. T. Gillen, "Radiation-Thermal Degradation of PE and PVC; Mechanism of Synergism and Dose Rate Effects," Rad. Phys. Chem. 18, 661-669 (1981).
- Egorov, E. V. and P. D. Novikov, Action of Ionizing Radiation on Ion-Exchange Material, Atomizdat, Moscow, 1965, Israel Program for Scientific Translations, Jerusalem, 1967.
- Gangwer, T. E., M. Goldstein, and K. K. S. Pillay, Brookhaven National Laboratory, "Radiation Effects on Ion-Exchange Materials," BNL 50781, November 1977.
- Gangwer, T. E., Brookhaven National Laboratory and K. K. S. Pillay, Pennsylvania State University, "Radioactive Loading of Ion-Exchange Materials: Radiation Related Areas of Concern," BNL-NUREG-28647, 1980.
- Gangwer, T. E. and K. K. S. Pillay, "Radiation-Induced Corrosion of Mild Steel in Contact With Ion-Exchange Materials," Nuclear Technology 58, 548, 1982.
- Godbee, H., Private Communication.
- Hovey, G. K., Metropolitan Edison Company, Memorandum to J. T. Collins, U. S. Nuclear Regulatory Commission, December 4, 1980.
- Kendig, M. W. and H. Isaacs, "Corrosion of Alloy 600 by Cationic Resin Beads," Nuclear Technology 55, 191, 1981.
- MacKenzie, D. R., M. Lin, and R. E. Barletta, Brookhaven National Laboratory Informal Report, "Permissible Radionuclide Loading for Organic Ion-Exchange Resins From Nuclear Power Plants," BNL-NUREG-30668, January 1982.
- Malinauskas, A., Oak Ridge National Laboratory, private communicaiton to G. P. Quinn, EGG/TMI, June 13, 1983.
- Mathur, J. W. and Vasudevan, "Reactivity Rate Studies for the Corrosion of Metals in Acids, I: Iron in Mineral Acids," Corrosion 38, 121-128, 1982.

- McFarland, R. C., Georgia Institute of Technology, "The Effects of Gamma Radiation on Ion-Exchange Resins and Activated Charcoal," TMI-II-RR-6, 1980. See also R. C. McFarland, "Analysis of Irradiated Ion-Exchange Materials, Rinal Research Report," Project A60-611, May 1981.
- Pillay, K. K. S., Pennsylvania State University, "Radiation Effects on Ion Exchanger Used in Radioactive Waste Management," NE-RWM-80-3, 1980.
- Scully, J. C., The Fundamentals of Corrosion, Pergamon Press, New York, 1975.
- Sheff, J. R., "Technical Approach to the interpretation of PF-Vessel Gas Test Data, GPU Memo, July 21, 1982; "Evaluation of PF Vessel 3 With Reference to Shipping," GPU Memo, August 6, 1982.
- Swyler, K. J. and R. E. Barletta, Brookhaven National Laboratory, "Irradiation of Zeolite Ion-Exchange Media," BNL-NUREG-51551, 1982.
- Swyler, K. J., C. J. Dodge, and R. Dayal, Brookhaven National Laboratory, "Irradiation Effects on the Storage and Disposal of Radwaste Containing Organic Ion-Exchange Media," BNL-NUREG-51691, 1983.
- Swyler, K. J., C. J. Dodge and R. Dayal, "Irradiation Effects on Ion Exchange Media," Materials Research Society Symposium Proceedings 15, 385, 1983.
- Uhlig, H. H., Corrosion Handbook, John Wiley and Sons, New York, 1948.
- Wynhoff, N. L., and J. Pasupathi, Battelle Columbus Laboratory, "Characterization of Epicor-II Prefilter Liner 3," GEND/EGG Report, GEND 027, April 1983.
- Yesso, J. D., V. Pasupathi, and L. Lowry, Battelle Columbus Laboratory, "Characterization of Epicor-II Prefilter Liner 16," GEND/EGG Report, GEND 015, August 1982.

OFFSITE DISTRIBUTION LIST

Battelle Columbus Laboratory
Project Management Division
505 King Ave.
Columbus, OH 43201

Attn: D. F. Clark

Battelle Columbus Laboratory
West Jefferson Site
505 King Ave.
Columbus, OH 43201

Attn: V. Pasupathi
H. Wynhoff

Chem Nuclear
240 Stoneridge Drive
Suite 100
Columbia, SC

Attn: J. Geoffrey
J. Staehr

Dow Chemical
Larkin Laboratory
1691 N. Swede Road
Midland, MI 48640

Attn: H. Filter
B. Owens

EG and G Idaho
PO Box 1625
Idaho Falls, ID 83415

Attn: S. Croney
J. W. Mandler
R. Ogle

OFFSITE DISTRIBUTION LIST (Continued)

EG and G/TMI Office
P.O. Box 88
Middletown, PA 17057

Attention: G. Quinn

Electric Power Research Institute
3421 Hillview Ave.
PO Box 10412
Palo Alto, CA 94301

Attn: M. E. Norton
R. F. Williams

GPU Nuclear
100 Interscience Parkway
Parsippany, NJ 07054

Attn: T. Gangwer

Hittman Nuclear Development Corp.
Oakland Ridge Industrial Park
Columbia, MD 21045

Attn: W. Phillips

Los Alamos Scientific Laboratory
Group Q4, Mail Stop 541
Los Alamos, NM 87545

Attn: K.K.S. Pillay

Oak Ridge National Laboratory
PO Box X
Oak Ridge, TN 37830

Attn: H. Godbee

OFFSITE DISTRIBUTION LIST (Continued)

Office of Nuclear Material Safety
and Safeguards
US Nuclear Regulatory Commission
Mail Stop 623 SS
Washington, DC 20555

Attn: M. Bell T. Johnson
 R. E. Browning L. Person
 L. Higginbotham R. J. Starmer
 K. C. Jackson

Office of Nuclear Regulatory Research
US Nuclear Regulatory Commission
Mail Stop 1130 SS
Washington, DC 20555

Attn: F. J. Arsenault K. Kim (10)
 G. F. Birchard M. McNeil
 E. F. Conti E. O'Donnell
 F. A. Costanzi

Pacific Northwest Laboratory
P.O. Box 999
Richland, WA 99352

Attn: J. H. Westsik, Jr.

University of Lowell
Lowell, MA 01854

Attention: J. Sheff

US Department of Energy
Germantown
Washington, DC 20545

Attn: E. Jordan

OFFSITE DISTRIBUTION LIST (Continued)

Waste Chem Corp
663 E. Crescent Ave.
Ramsey, NJ 07446

Attn: S. R. Beck
D. N. Enegess
W. Klein

BROOKHAVEN NATIONAL LABORATORY

T. M. Ahn	H.J.C. Kouts
C. Anderson	S. G. Lane
H. Arora	C. Pescatore
R. E. Barletta	A. J. Romano
W. W. Becker	C. Sastre
P. Colombo	D. G. Schweitzer
M. S. Davis	P. Soo
R. E. Davis	K. J. Swyler
R. Dayal	H. Todosow
C. Dodge	J. Weeks
B. Karlin	A. J. Weiss
W. Y. Kato	

U.S. NUCLEAR REGULATORY COMMISSION
BIBLIOGRAPHIC DATA SHEET

1. REPORT NUMBER (Assigned by NRC)

NUREG/CR-3812
BNL-NUREG-51774

4. TITLE AND SUBTITLE (Add Volume No., if appropriate)
"Assessment of Irradiation Effects in Radwaste Containing Organic Ion-Exchange Media"

2. (Leave blank)
3. RECIPIENT'S ACCESSION NO.

7. AUTHOR(S)
K. J. Swyler, C. J. Dodge and R. Dayal

6. DATE REPORT COMPLETED
MONTH: March | YEAR: 1984

9. PERFORMING ORGANIZATION NAME AND MAILING ADDRESS (Include Zip Code)
Department of Nuclear Energy
Brookhaven National Laboratory
Upton, New York 11973

DATE REPORT ISSUED
MONTH: | YEAR:
7. (Leave blank)
8. (Leave blank)

12. SPONSORING ORGANIZATION NAME AND MAILING ADDRESS (Include Zip Code)
Division of Regulatory Research
U. S. Nuclear Regulatory Commission
Washington, DC 20555

10. PROJECT/TASK/WORK UNIT NO.
11. FIN NO.
A-3236

13. TYPE OF REPORT
Technical Report

PERIOD COVERED (Inclusive dates)

15. SUPPLEMENTARY NOTES

14. (Leave blank)

16. ABSTRACT (200 words or less)
Recently, regulatory consideration has been devoted to the effects of self-irradiation on radwaste containing organic ion exchange media. This consideration was prompted by decontamination operations at TMI-II, and by the development of technical positions in support of NRC regulation 10 CFR 60. This report addresses the effects of high radiation dose on the storage and disposal of radwaste ion-exchange media, and the validity of laboratory test procedures for predicting field performance. Our work shows that accelerated testing of ion-exchange media using high-dose-rate external gamma irradiation appears to be a valid procedure for assessing certain aspects of field behavior--i.e. radiolytic scission of the resin functional group, radiolytic gas generation of free liquids and resin agglomeration, provided both the test data and the field conditions refer to storage in a closed environment. Certain resin decomposition processes appear to depend largely on resin moisture content, and may not be particularly sensitive to resin loading. One practical consequence of radiolytic acidity is to promote the corrosion of mild steel in irradiated resin. However, the corrosion process is very complex. Case-specific, long-term (i.e. low radiation dose) evaluations might be necessary if rigorous guidelines to protect radwaste containers against corrosion are required.

17. KEY WORDS AND DOCUMENT ANALYSIS
radioactive waste disposal, ion-exchange media, radiation effects, resin degradation products, mild steel corrosion, laboratory test procedures

17a. DESCRIPTORS

17b. IDENTIFIERS/OPEN ENDED TERMS

18. AVAILABILITY STATEMENT
UNLIMITED

19. SECURITY CLASS (This report)
unclassified
20. SECURITY CLASS (This page)

21. NO. OF PAGES
22. PRICE

120555078877 1 IANIRW
US NRC
ADM-DIV OF TIDC
POLICY & PUB MGT BR-PDR NUREG
W-501
WASHINGTON DC 20555